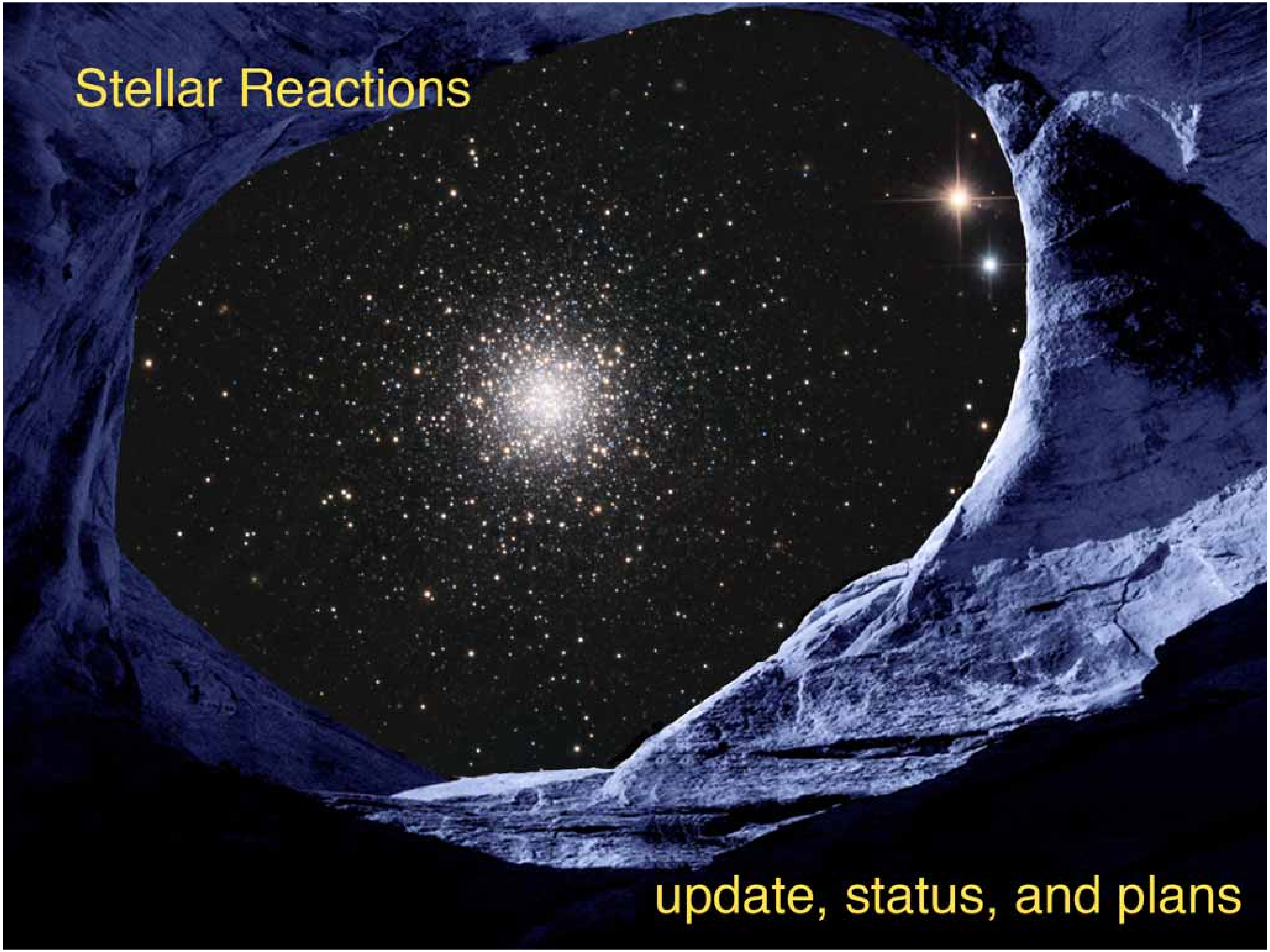
Stellar Reactions
update, status, and plans

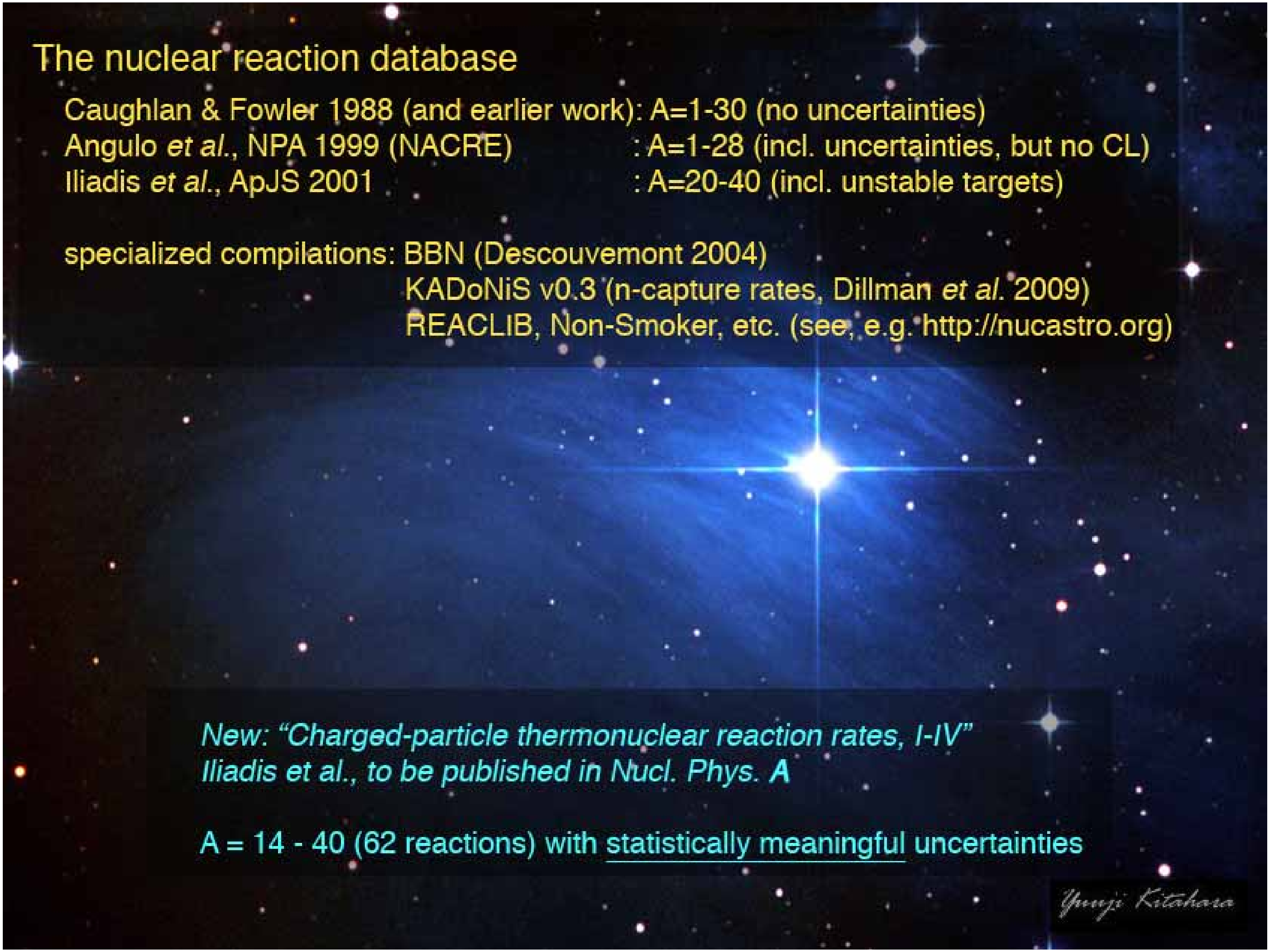

The nuclear reaction database

Caughlan & Fowler 1988 (and earlier work): A=1-30 (no uncertainties)
Angulo *et al.*, NPA 1999 (NACRE) : A=1-28 (incl. uncertainties, but no CL)
Iliadis *et al.*, ApJS 2001 : A=20-40 (incl. unstable targets)

specialized compilations: BBN (Descouvemont 2004)
KADoNiS v0.3 (n-capture rates, Dillman *et al.* 2009)
REACLIB, Non-Smoker, etc. (see, e.g. http://nucastro.org)

New: "Charged-particle thermonuclear reaction rates, I-IV"
Iliadis et al., to be published in Nucl. Phys. ***A***

A = 14 - 40 (62 reactions) with statistically meaningful uncertainties

Monte Carlo method: for 62 reactions from ^{14}C to ^{40}Ca target nuclei

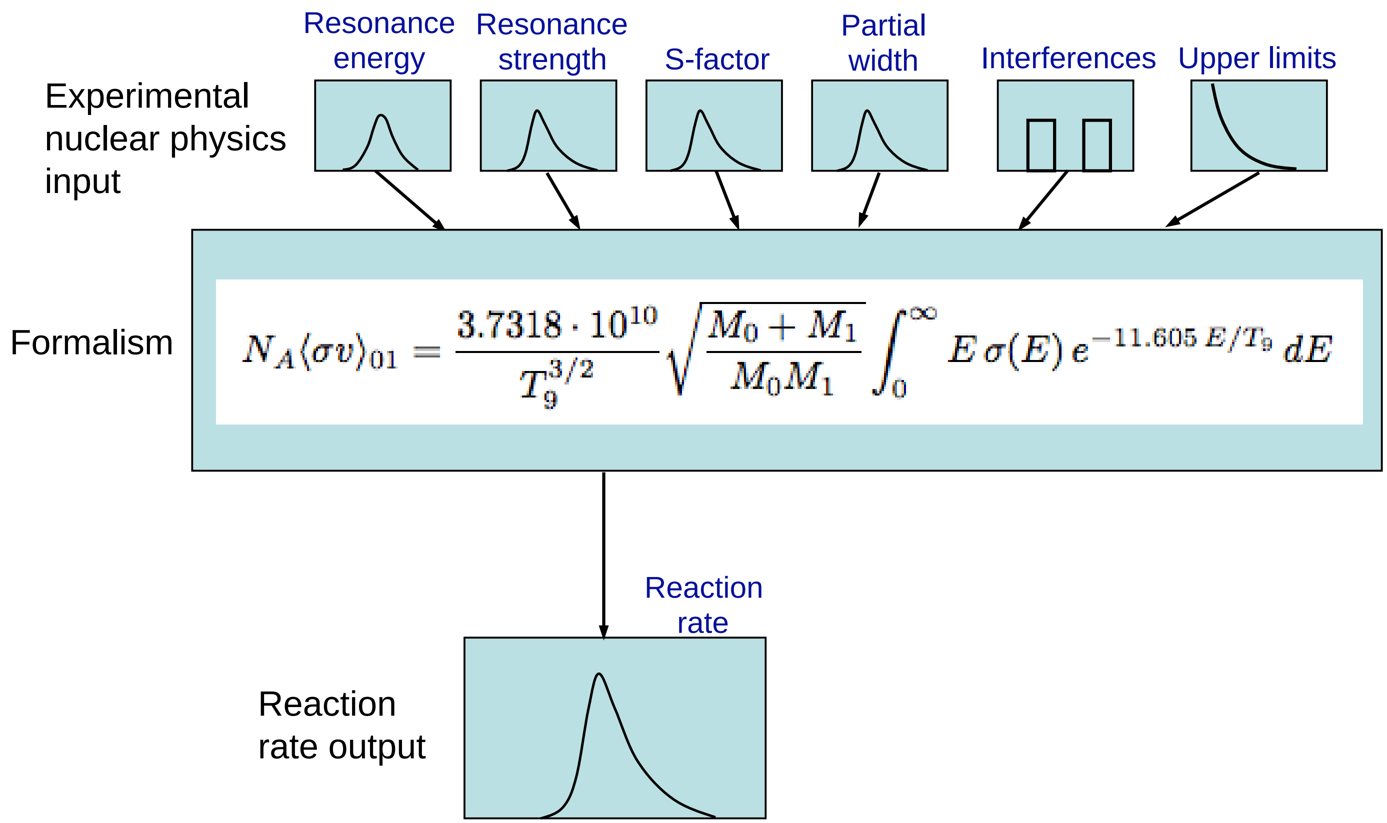

$$N_A\langle\sigma v\rangle_{01} = \frac{3.7318\cdot 10^{10}}{T_9^{3/2}}\sqrt{\frac{M_0+M_1}{M_0 M_1}}\int_0^\infty E\,\sigma(E)\,e^{-11.605\,E/T_9}\,dE$$

We find that majority of rates have a lognormal probability density function:

$$f(x>0) = \frac{1}{\sigma\sqrt{2\pi}}\frac{1}{x}e^{-(\ln x-\mu)^2/(2\sigma^2)}$$

plots of f(x) for 20,000 samples:

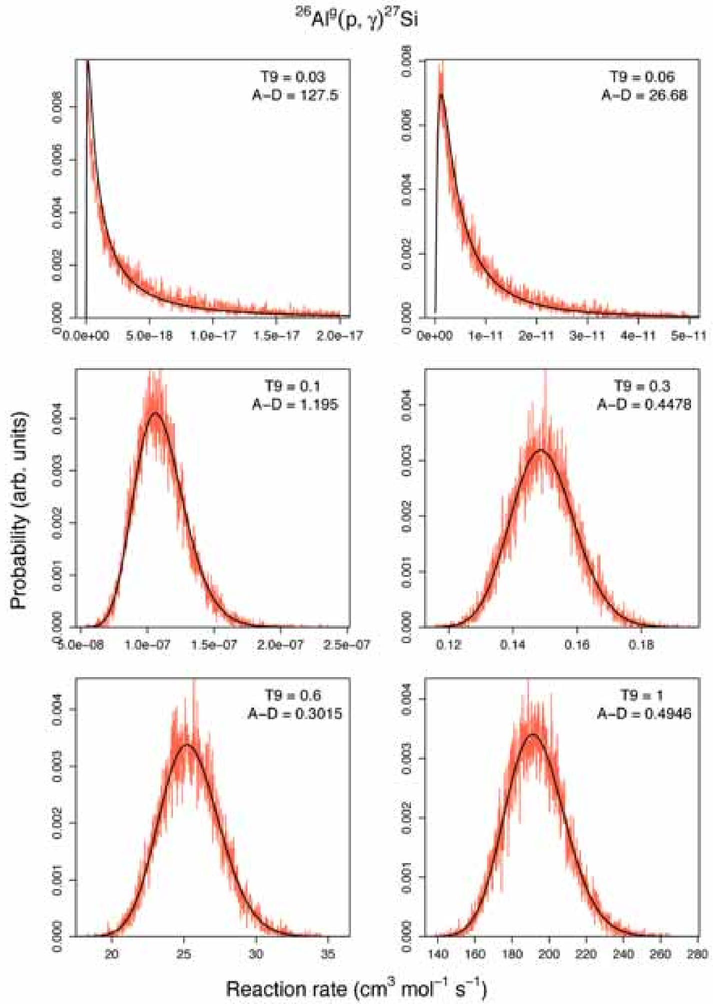

new library to be released this fall

Table B.31: Total thermonuclear reaction rates for $^{27}Al(p,\gamma)^{28}Si$.

T (GK)	Low rate	Median rate	High rate	lognormal μ	lognormal σ	A-D
0.010	3.30×10^{-37}	4.88×10^{-37}	7.14×10^{-37}	$-8.361\times10^{+01}$	3.87×10^{-01}	5.26×10^{-01}
0.011	9.13×10^{-36}	1.35×10^{-35}	1.96×10^{-35}	$-8.030\times10^{+01}$	3.84×10^{-01}	9.71×10^{-01}
0.012	1.70×10^{-34}	2.50×10^{-34}	3.66×10^{-34}	$-7.737\times10^{+01}$	3.86×10^{-01}	2.42×10^{-01}
0.013	2.38×10^{-33}	3.46×10^{-33}	5.03×10^{-33}	$-7.474\times10^{+01}$	3.78×10^{-01}	2.42×10^{-01}
0.014	2.81×10^{-32}	4.11×10^{-32}	5.87×10^{-32}	$-7.228\times10^{+01}$	3.68×10^{-01}	$1.84\times10^{+00}$
0.015	2.92×10^{-31}	4.74×10^{-31}	7.59×10^{-31}	$-6.983\times10^{+01}$	4.65×10^{-01}	$2.42\times10^{+00}$
0.016	2.70×10^{-30}	5.76×10^{-30}	1.33×10^{-29}	$-6.730\times10^{+01}$	7.34×10^{-01}	$2.53\times10^{+01}$
0.018	1.84×10^{-28}	9.75×10^{-28}	2.96×10^{-27}	$-6.237\times10^{+01}$	$1.23\times10^{+00}$	$8.16\times10^{+01}$
0.020	1.31×10^{-26}	8.04×10^{-26}	2.51×10^{-25}	$-5.803\times10^{+01}$	$1.37\times10^{+00}$	$9.57\times10^{+01}$
0.025	6.60×10^{-23}	2.65×10^{-22}	7.48×10^{-22}	$-4.987\times10^{+01}$	$1.26\times10^{+00}$	$8.05\times10^{+01}$
0.030	2.03×10^{-20}	7.00×10^{-20}	1.60×10^{-19}	$-4.431\times10^{+01}$	$1.14\times10^{+00}$	$1.27\times10^{+02}$
0.040	2.41×10^{-17}	8.33×10^{-17}	1.68×10^{-16}	$-3.728\times10^{+01}$	$1.09\times10^{+00}$	$1.92\times10^{+02}$
0.050	1.59×10^{-15}	5.64×10^{-15}	1.29×10^{-14}	$-3.303\times10^{+01}$	$1.13\times10^{+00}$	$1.51\times10^{+02}$
0.060	2.95×10^{-14}	9.66×10^{-14}	2.43×10^{-13}	$-3.010\times10^{+01}$	$1.02\times10^{+00}$	$7.66\times10^{+01}$
0.070	9.71×10^{-13}	1.50×10^{-12}	2.69×10^{-12}	$-2.717\times10^{+01}$	4.59×10^{-01}	$5.65\times10^{+01}$
0.080	3.78×10^{-11}	4.44×10^{-11}	5.22×10^{-11}	$-2.384\times10^{+01}$	1.60×10^{-01}	9.78×10^{-01}
0.090	7.61×10^{-10}	8.64×10^{-10}	9.84×10^{-10}	$-2.087\times10^{+01}$	1.31×10^{-01}	7.53×10^{-01}
0.100	8.71×10^{-09}	9.79×10^{-09}	1.10×10^{-08}	$-1.844\times10^{+01}$	1.19×10^{-01}	5.99×10^{-01}
0.110	6.44×10^{-08}	7.16×10^{-08}	7.98×10^{-08}	$-1.645\times10^{+01}$	1.08×10^{-01}	4.73×10^{-01}
0.120	3.40×10^{-07}	3.76×10^{-07}	4.15×10^{-07}	$-1.479\times10^{+01}$	1.00×10^{-01}	4.00×10^{-01}
0.130	1.39×10^{-06}	1.52×10^{-06}	1.67×10^{-06}	$-1.339\times10^{+01}$	9.37×10^{-02}	3.28×10^{-01}
0.140	4.64×10^{-06}	5.06×10^{-06}	5.51×10^{-06}	$-1.219\times10^{+01}$	8.82×10^{-02}	2.85×10^{-01}
0.150	1.32×10^{-05}	1.43×10^{-05}	1.55×10^{-05}	$-1.116\times10^{+01}$	8.34×10^{-02}	3.08×10^{-01}
0.160	3.28×10^{-05}	3.55×10^{-05}	3.84×10^{-05}	$-1.025\times10^{+01}$	7.92×10^{-02}	3.42×10^{-01}
0.180	1.52×10^{-04}	1.63×10^{-04}	1.75×10^{-04}	$-8.721\times10^{+00}$	7.17×10^{-02}	3.14×10^{-01}
0.200	5.26×10^{-04}	5.61×10^{-04}	5.98×10^{-04}	$-7.485\times10^{+00}$	6.47×10^{-02}	2.39×10^{-01}
0.250	5.44×10^{-03}	5.71×10^{-03}	5.99×10^{-03}	$-5.166\times10^{+00}$	4.89×10^{-02}	5.28×10^{-01}
0.300	2.97×10^{-02}	3.08×10^{-02}	3.20×10^{-02}	$-3.479\times10^{+00}$	3.76×10^{-02}	4.99×10^{-01}

16% — 50% — 84% of cumulative distribution

$e^{\mu-\sigma}$ — e^{μ} — $e^{\mu+\sigma}$

new data

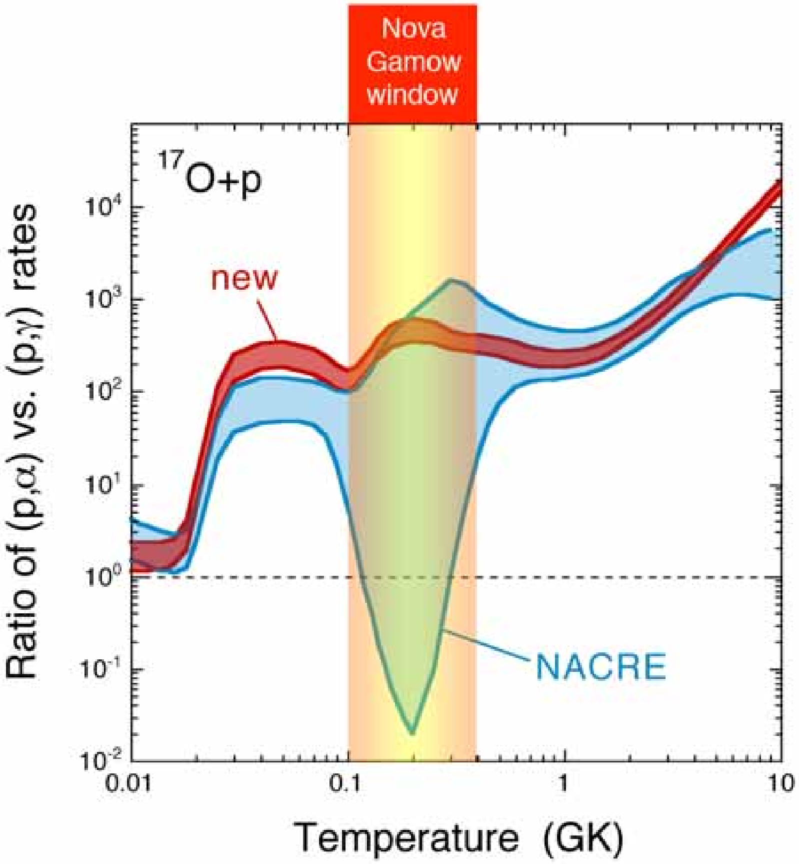

Fox *et al.*, *Phys. Rev. C* **71**, 055801 (2005)
Chafa *et al.*, *Phys. Rev. C* **75**, 035810 (2007)
Newton *et al.*, *Phys. Rev. C* **81**, 045801 (2010)

new statistical analysis

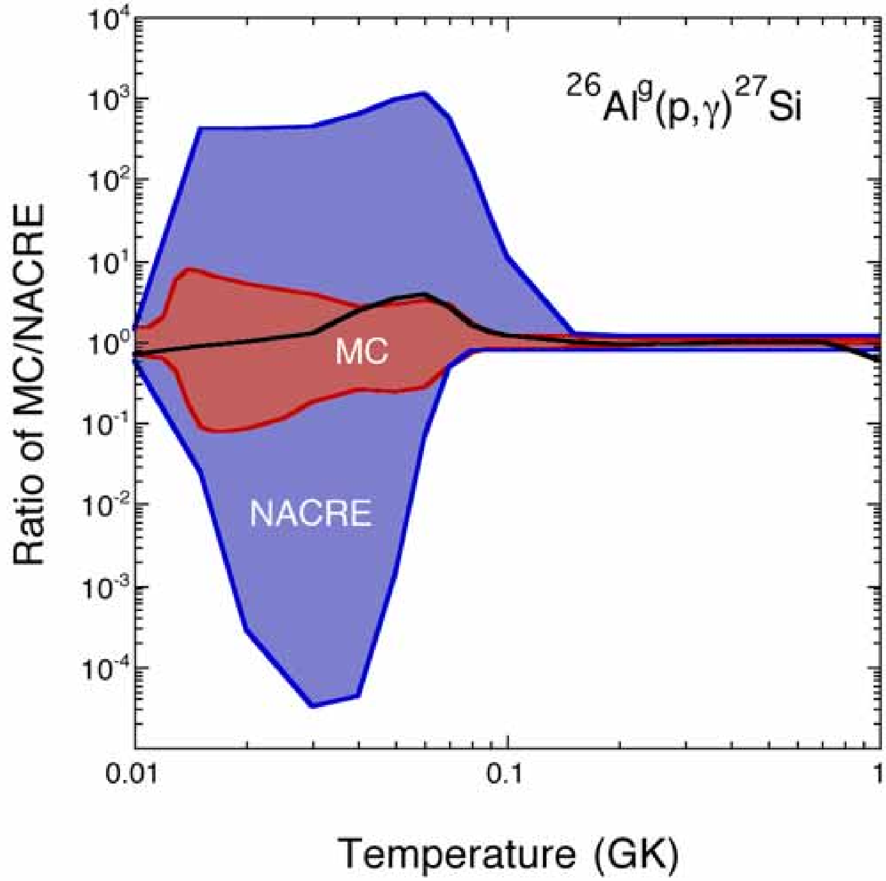

Ages of globular clusters

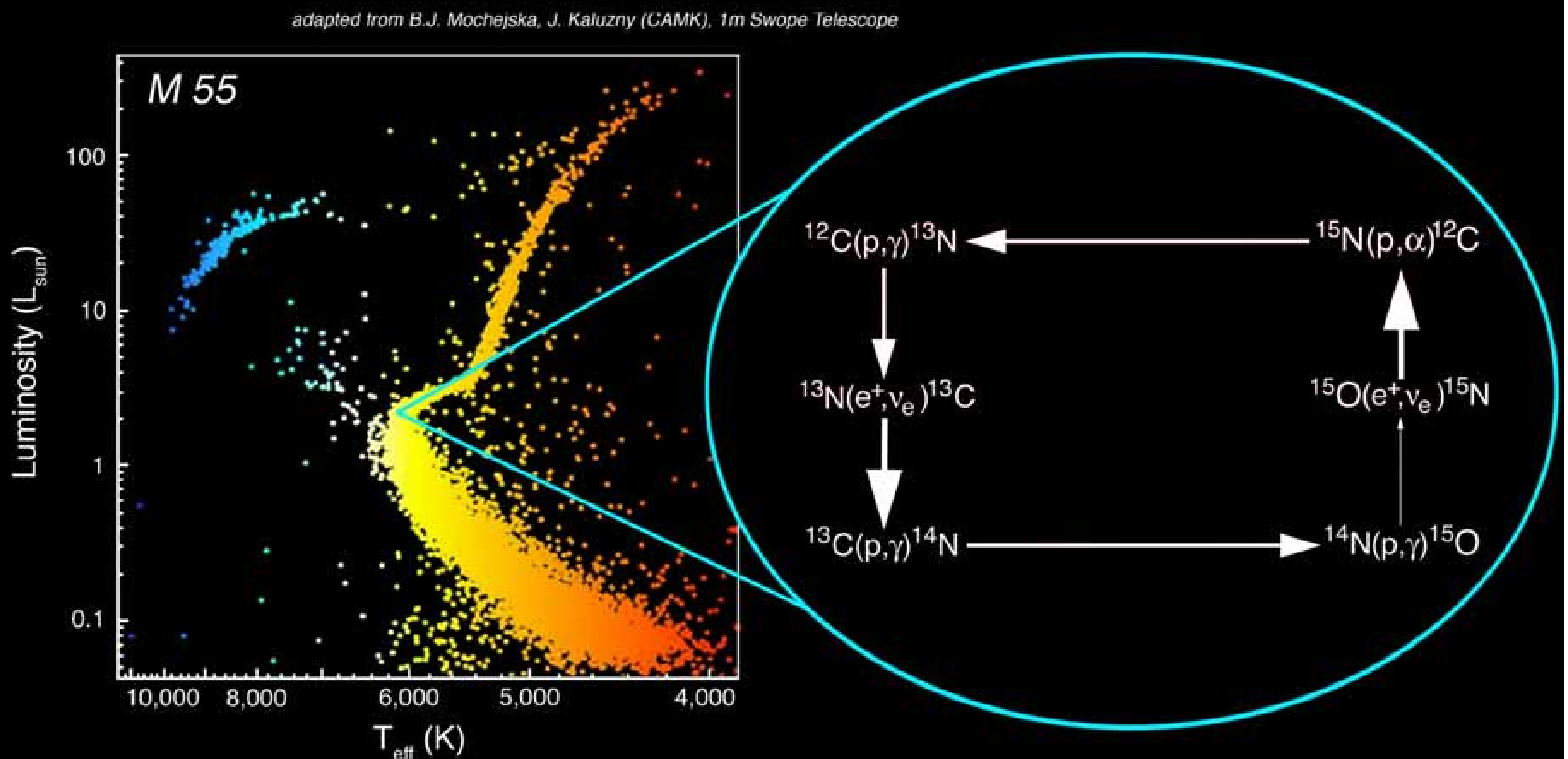

How reliable is the reaction model?

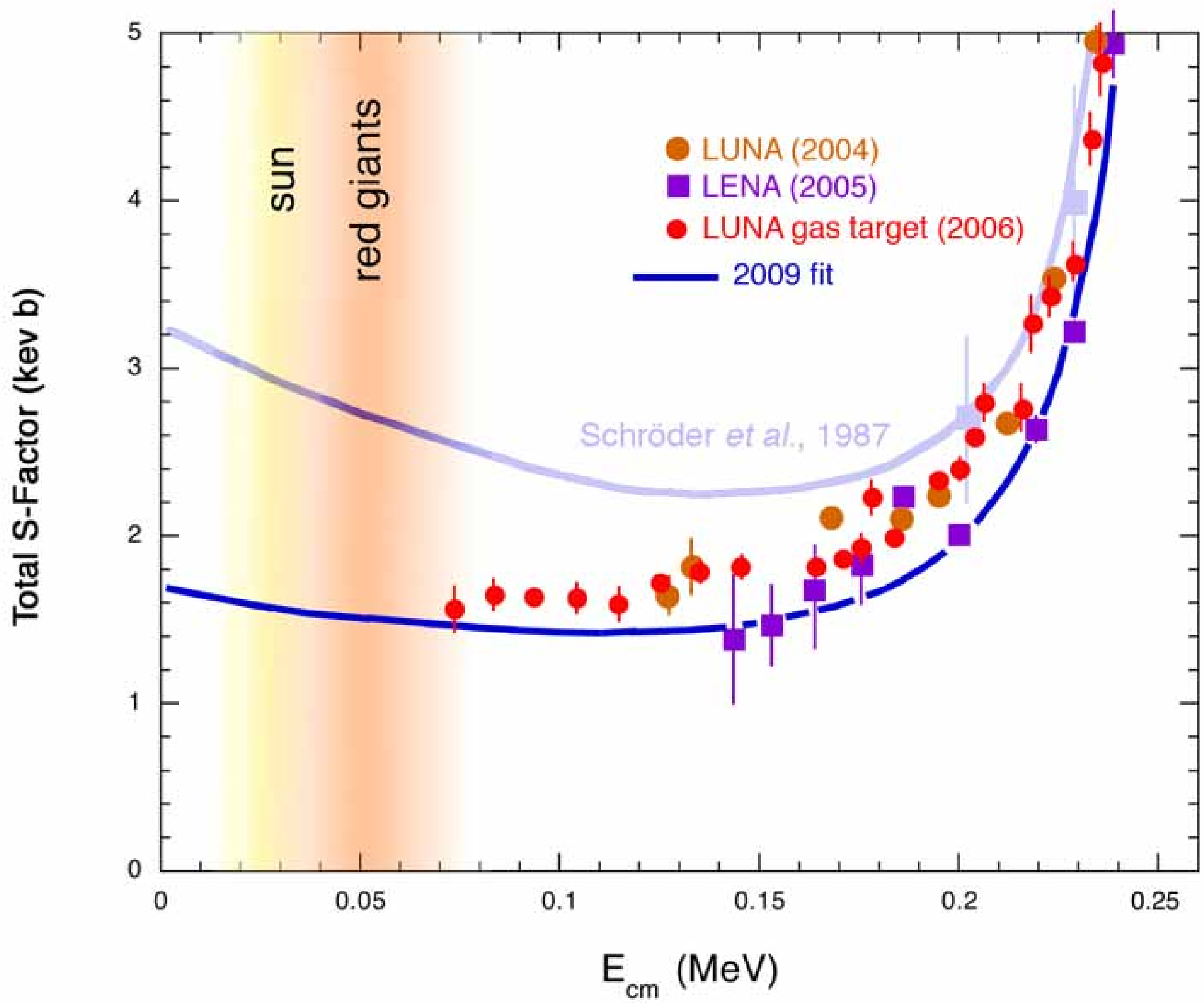

factor of 6.7 x 10^{13}
in cross section

How reliable is the reaction model?

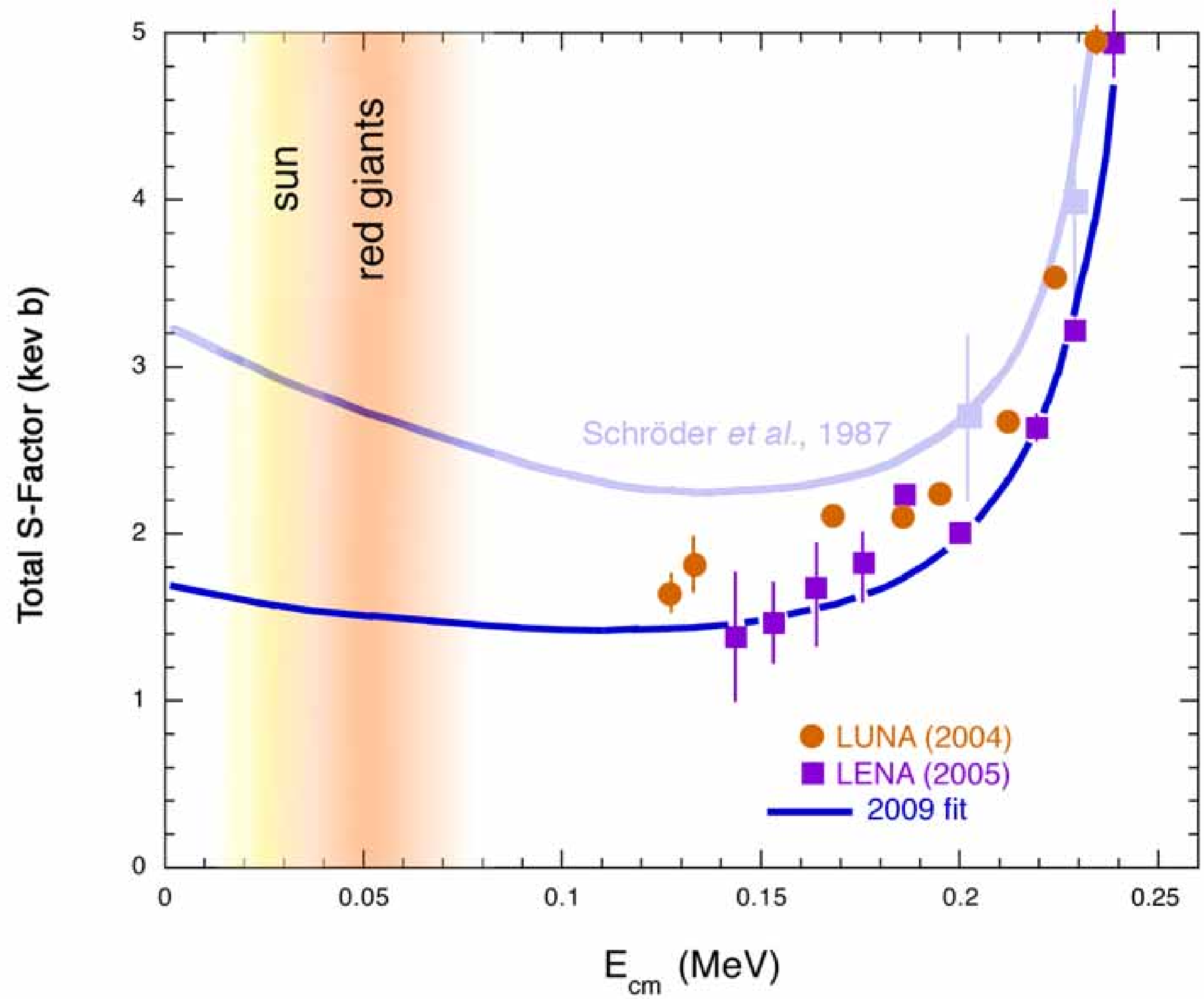

factor of 6.7 x 10^{13}
in cross section

combined R-matrix fits
(solar fusion evaluation,
2010)

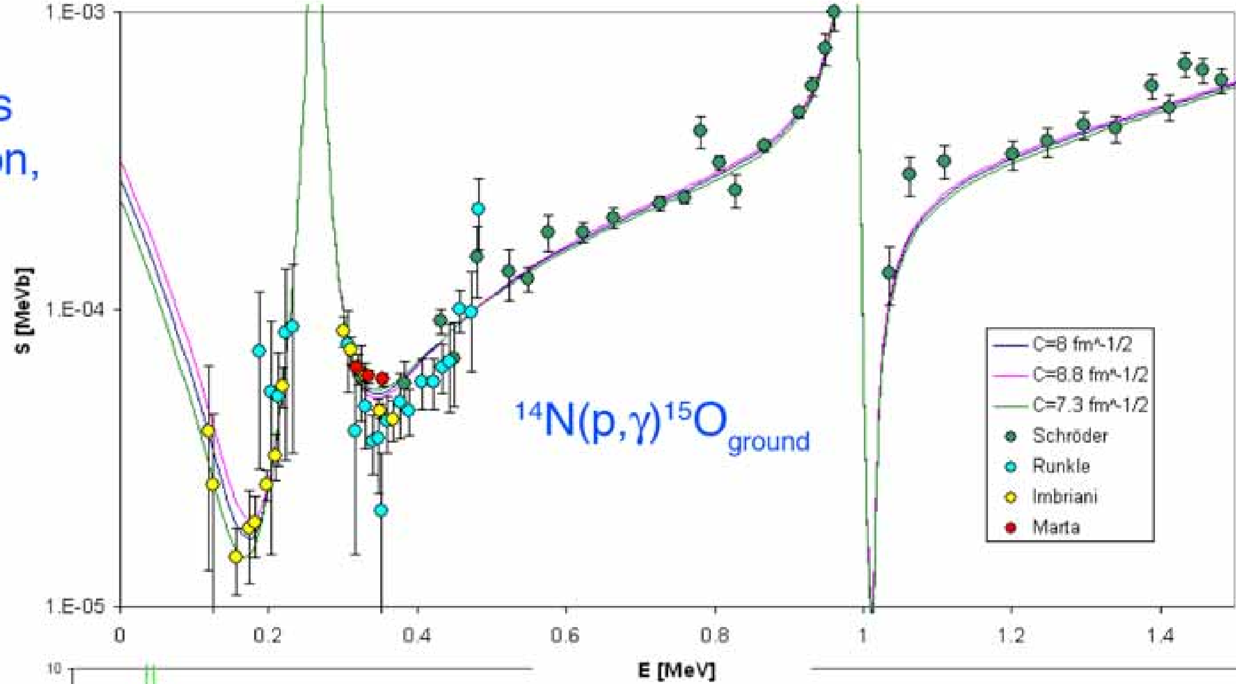

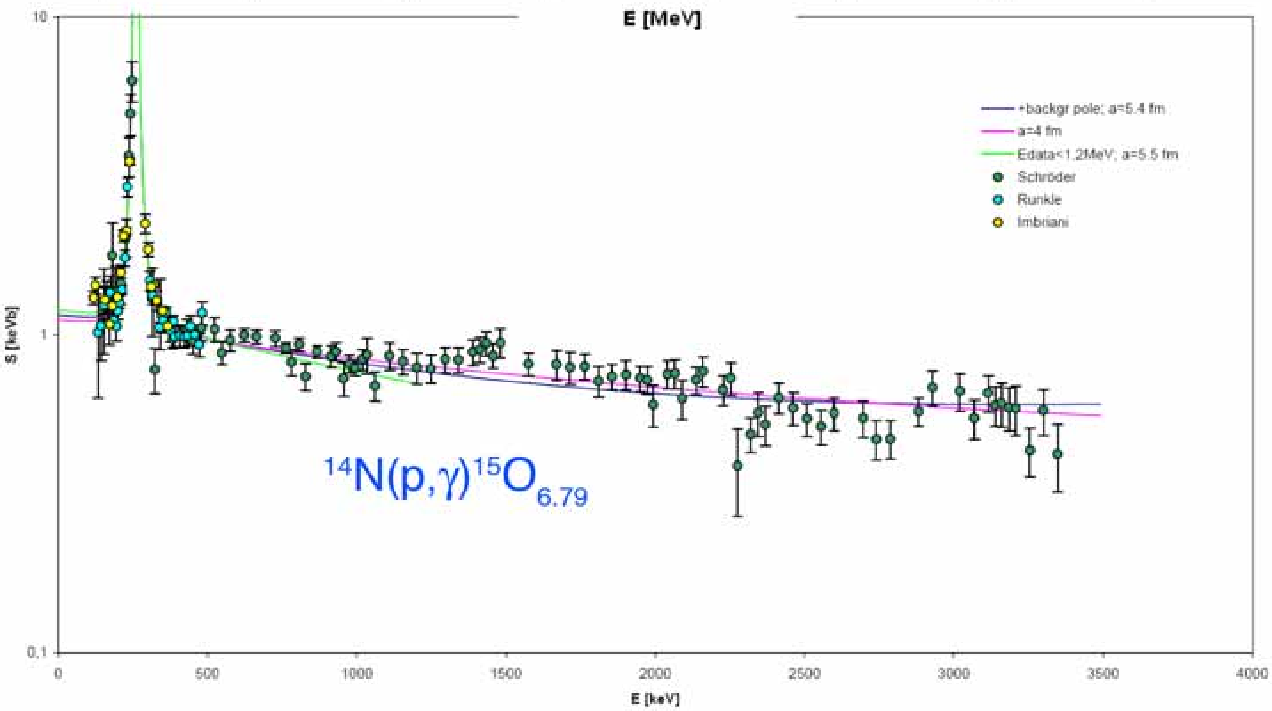

The situation in 2004-2005

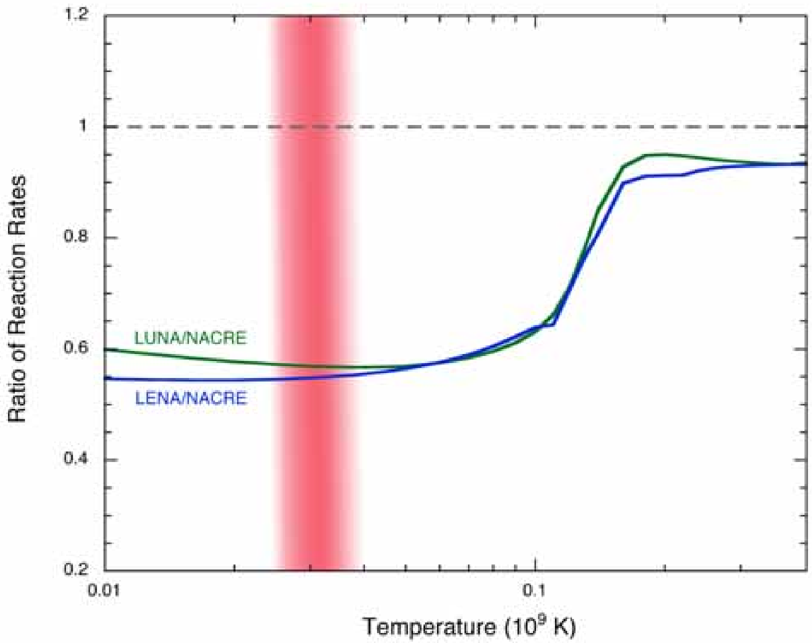

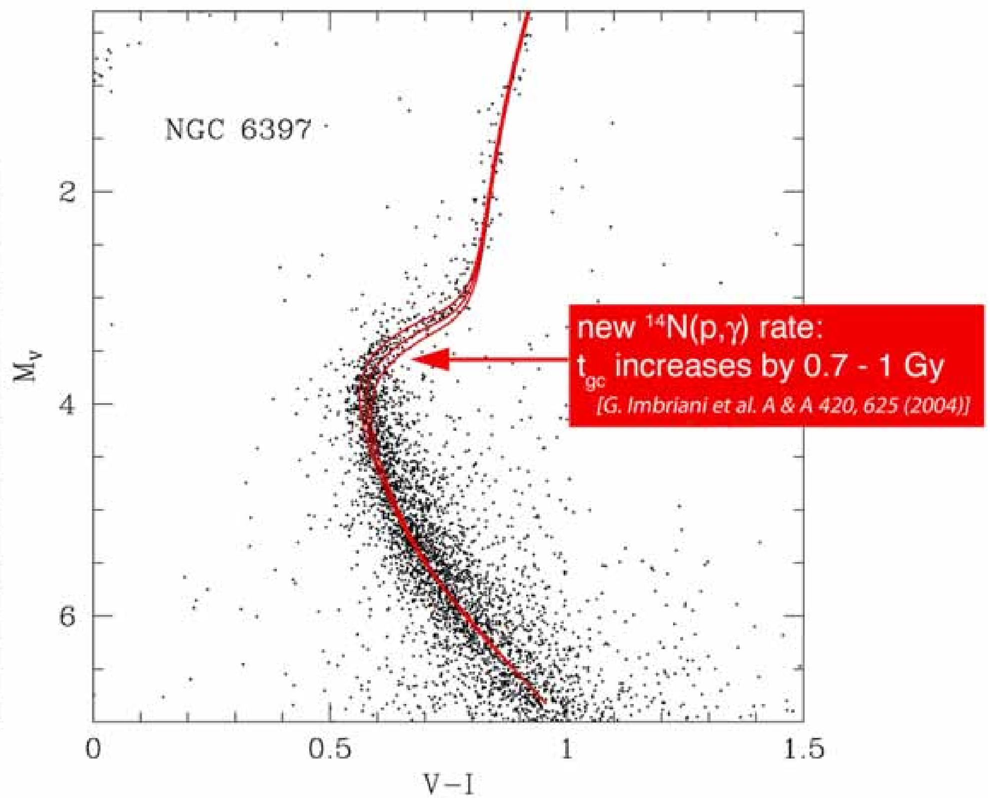

best-fit age ≈13.4 Gy

combined (p,p) and (p,γ) fits

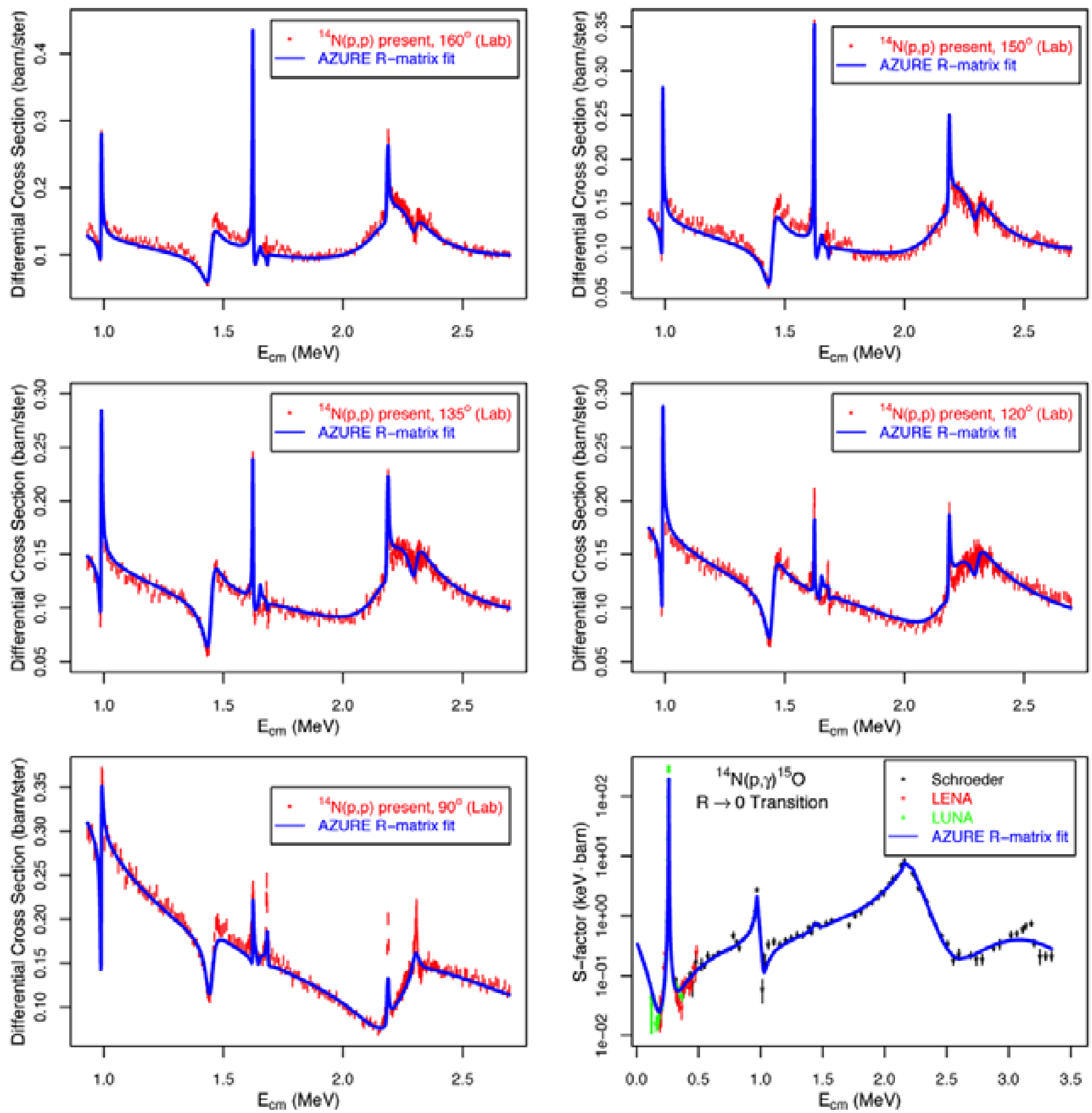

P. Bertone, PhD thesis (2010)


$^{12}C(\alpha,\gamma)$
$^{7}Be(p,\gamma)$
BAR

effect of $^{12}C(\alpha,\gamma)$ in massive stars (some examples)

supernovae

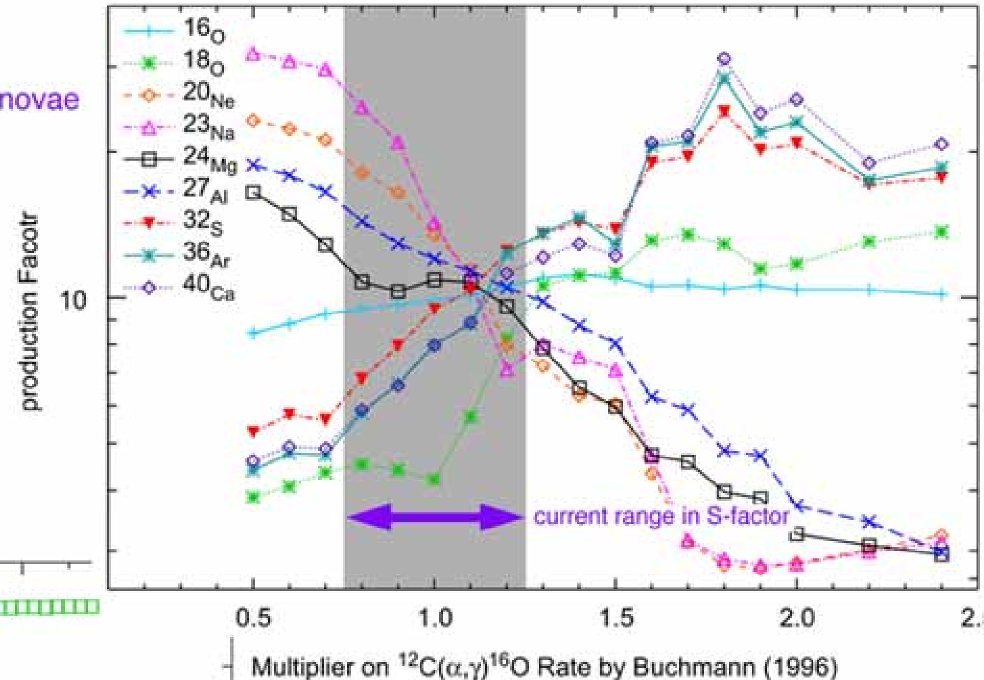

pre-supernova evolution

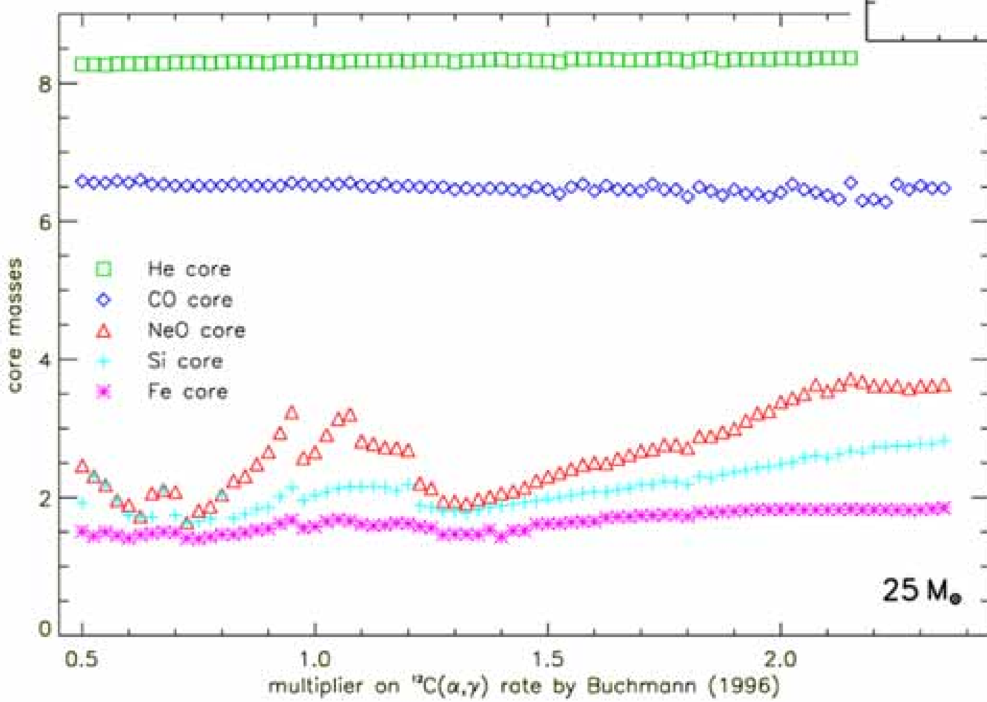

S.E. Woosley and A. Heeger, Phys. Rep. ***442****, 269 (2007)*
and M. Boyse, senior thesis, U.C. Santa Cruz (2002)
(http://www.supersci.org/data/nucleo/12cag/index.html)

also: chemical composition of white dwarfs, propagation of deflagration front in SNIa, etc.

$^{12}C(\alpha,\gamma)^{16}O$

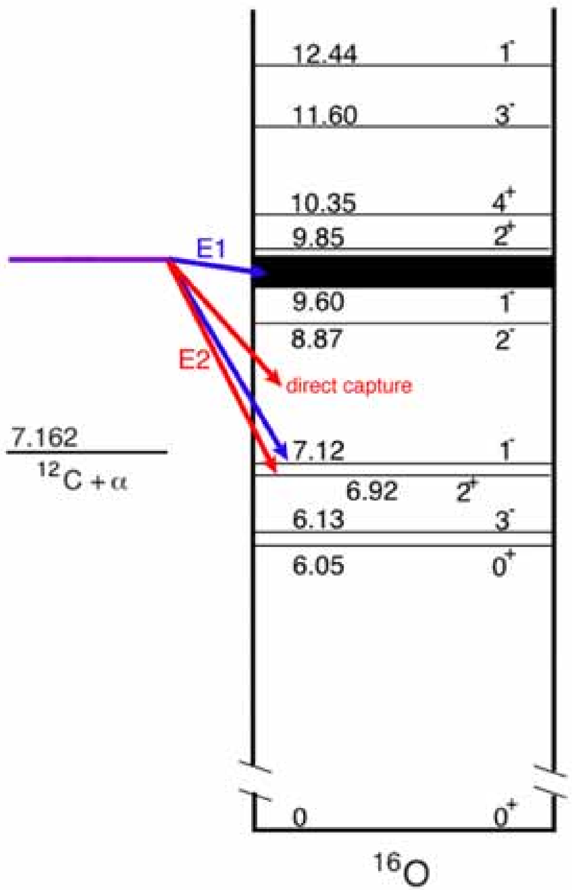

must also include interference with tails of distant 1^- and 2^+ states

recent capture data and R-matrix fits

J. Phys. G: Nucl. Part. Phys. **35** (2008) 014009 F Strieder

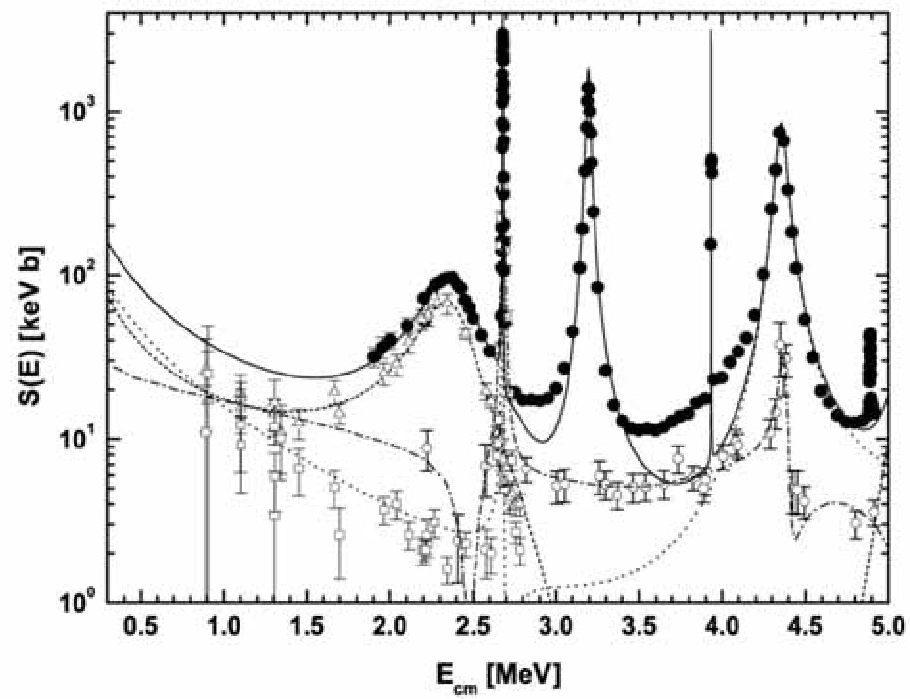

S(300) = 145 keV b ± ~25%

[L.R. Buchmann and C.A. Barnes, Nucl. Phys. **A 777,** 256 (2006)]

complementary approaches (e.g. elastic scattering, β-delayed α-decay of ^{16}N, etc.)

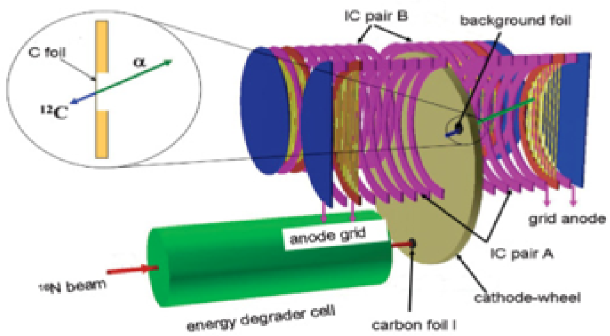

(a)

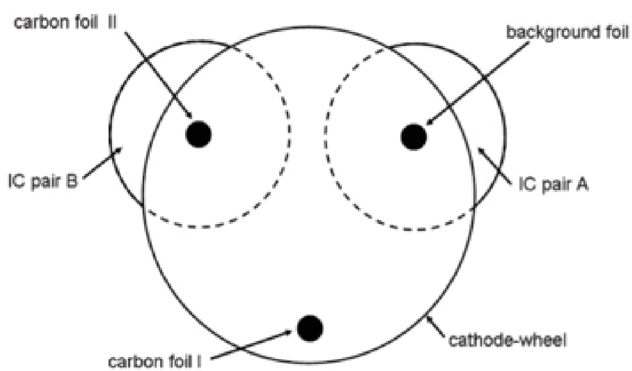

(b)

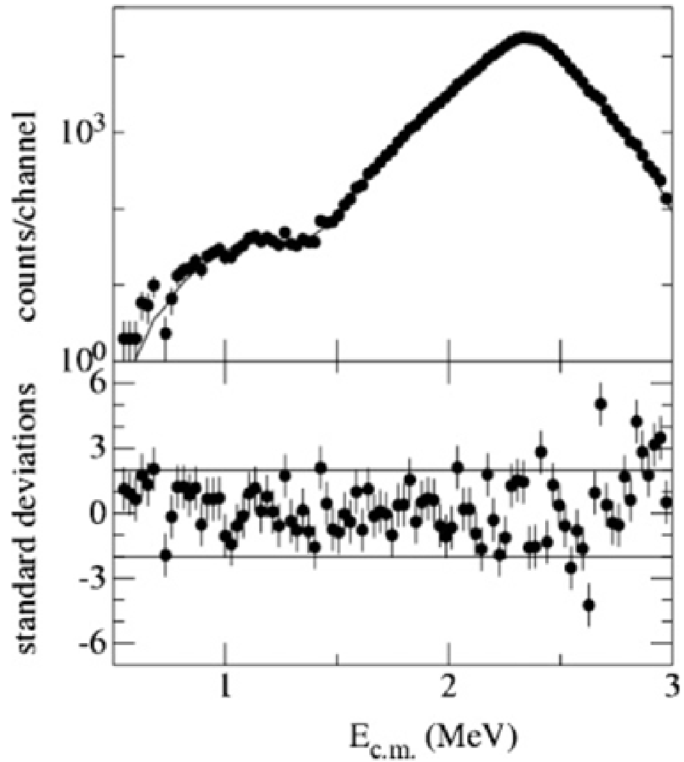

TABLE III. $S(E1)$ and $S(E2)$ values obtained by various experiments performed since 1994.

$S(E1)$ keVb	$S(E2)$ keVb	Ref.
86 ± 22		This work
	53 ± 16	[19]
79 ± 21		[21]
95 ± 44		[55]
101 ± 17	42 ± 20	[20]
76 ± 20	85 ± 30	[17]
77 ± 19	80 ± 25	[8]
81 ± 17		[10]
74 ± 21		[27]

X.D. Tang et al., Phys. Rev. C **81**, 045809 (2010)

$^{16}O(\gamma,\alpha)$ at HIγS*

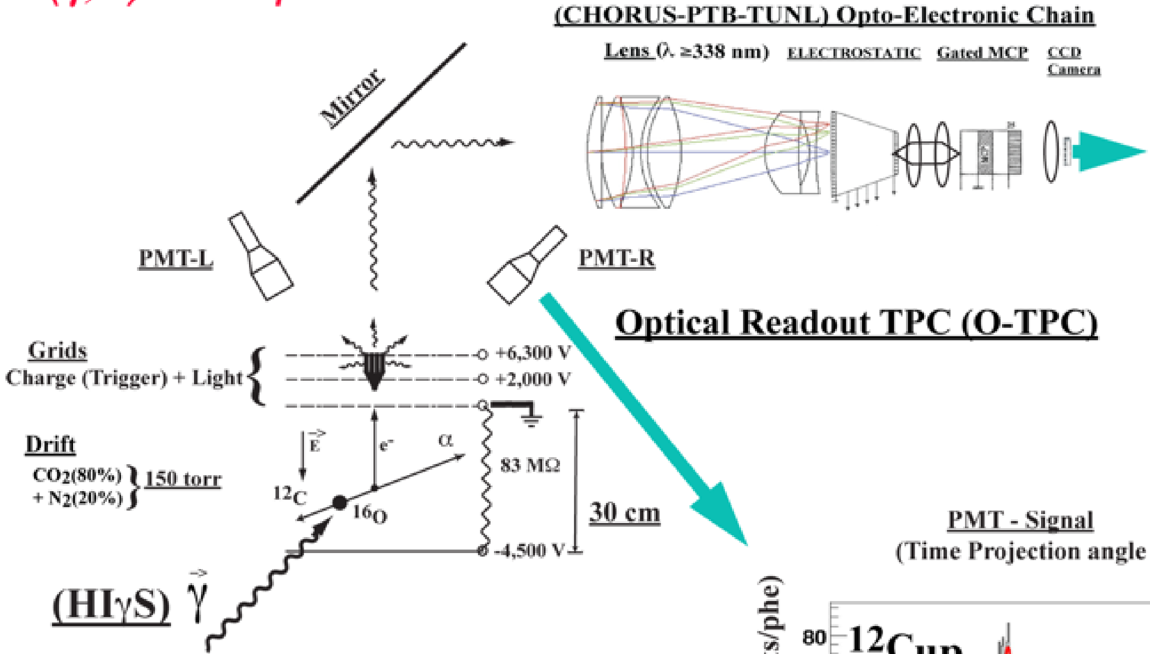

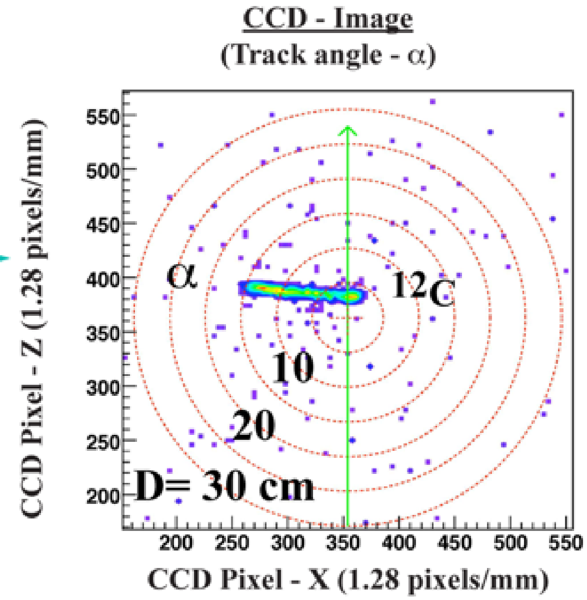

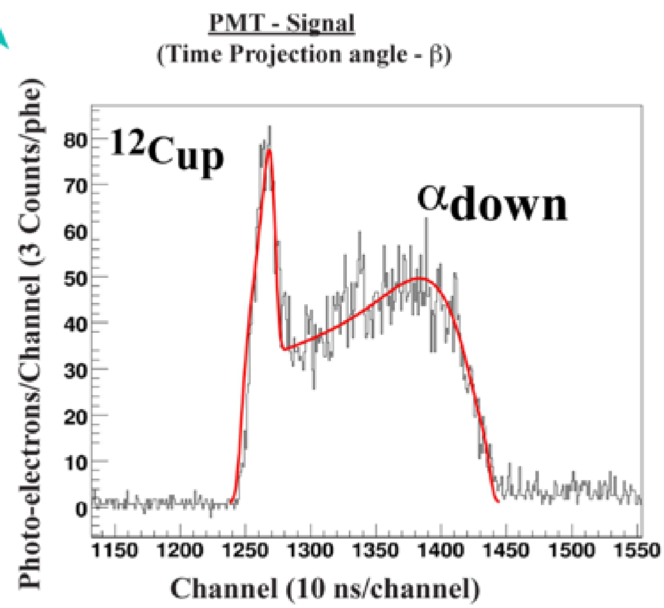

*collaboration involving TUNL,
Univ. of Connecticut,
Weizmann Inst.,
PTB, Braunschweig,
Yale Univ.,
Université catholique de Louvain,
Louvain-la-Neuve,
Univ. of Massachusetts,
Univ. of Hartford,
Georgia College and State Univ.,
North Georgia College and State Univ.

$^{16}O(\gamma,\alpha)$ at HIγS* - STAR (Superheated Target for Astrophysics Research)

*collaboration involving
Argonne
Fermilab
TUNL
Univ. of Chicago

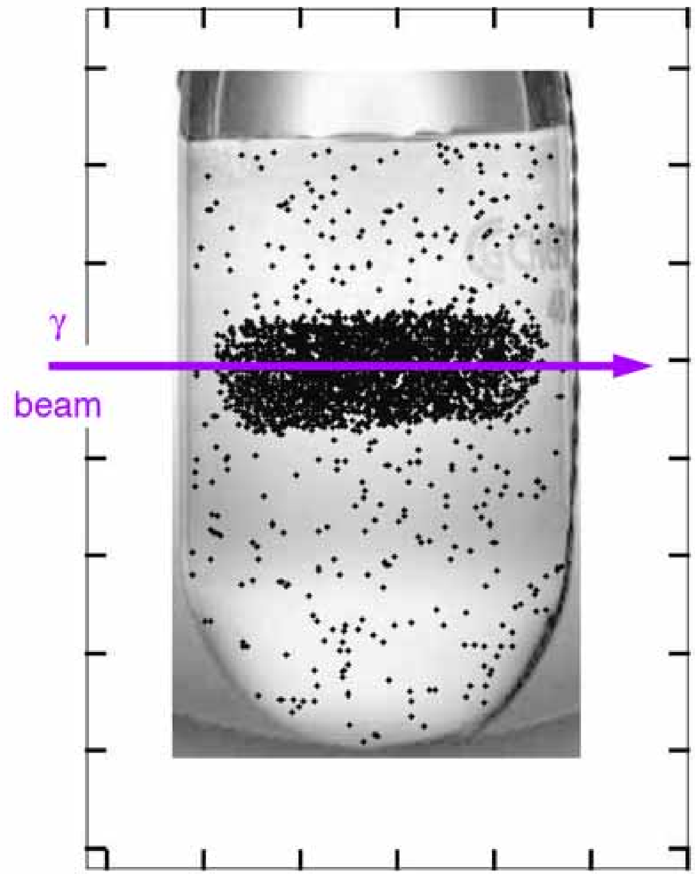

$^{19}F(\gamma,\alpha)$ events over 12 hrs
at 4×10^3 γ/s

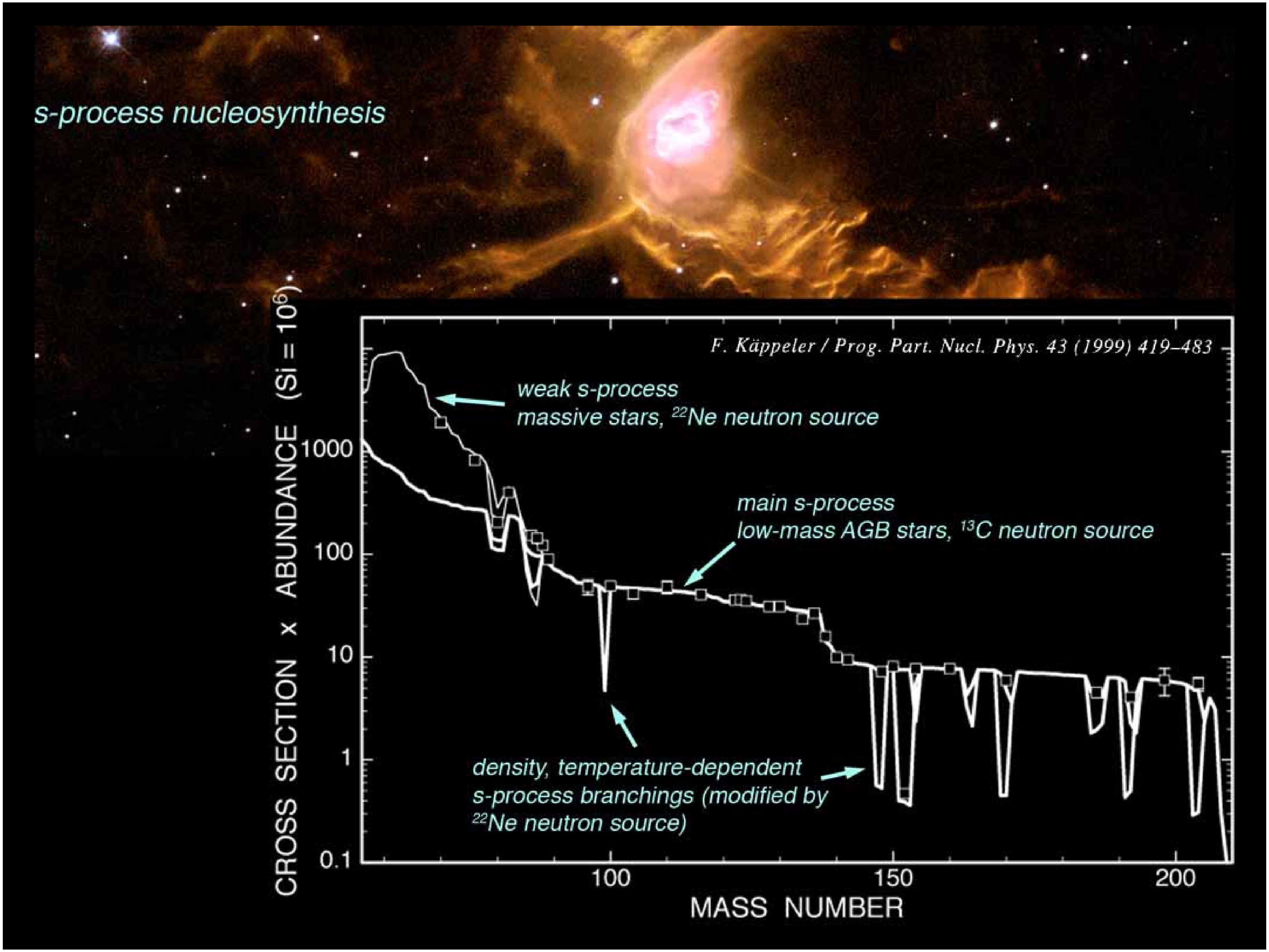
s-process nucleosynthesis
F. Käppeler / Prog. Part. Nucl. Phys. 43 (1999) 419–483
weak s-process
massive stars, ^{22}Ne neutron source
main s-process
low-mass AGB stars, ^{13}C neutron source
density, temperature-dependent
s-process branchings (modified by
^{22}Ne neutron source)
CROSS SECTION x ABUNDANCE (Si = 10^6)
MASS NUMBER
0.1
1
10
100
1000
100
150
200

Issues:

1. $^{13}C(\alpha,n)$ source: ^{13}C pocket is consistent with observations, but it does not arise naturally from standard AGB models

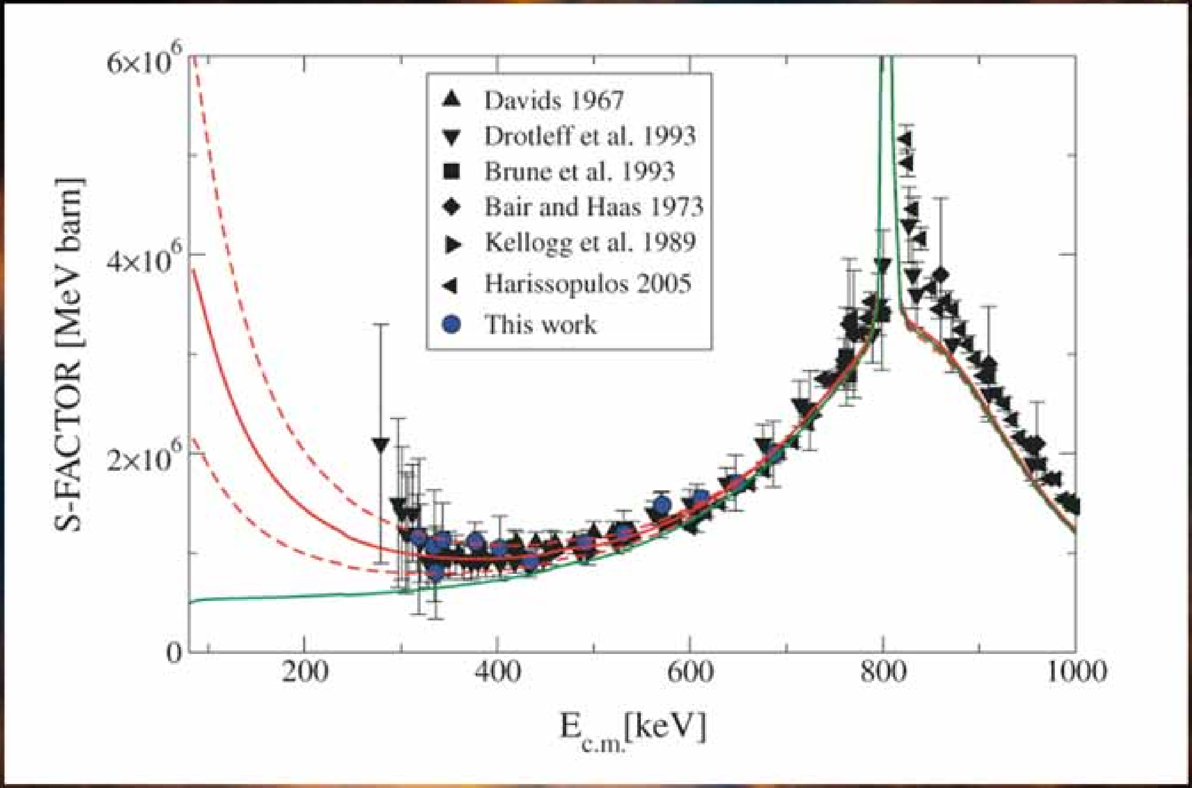

M. HEIL *et al.* PHYSICAL REVIEW C **78**, 025803 (2008)

Issues: 1. $^{13}C(\alpha,n)$ source: ^{13}C pocket is consistent with observations, but it does not arise naturally from standad AGB models

2. $^{22}Ne(\alpha,n)$ source: net neutron production is uncertain

$^{22}Ne(\alpha,n)^{25}Mg$ vs. $^{22}Ne(\alpha,\gamma)^{26}Mg$

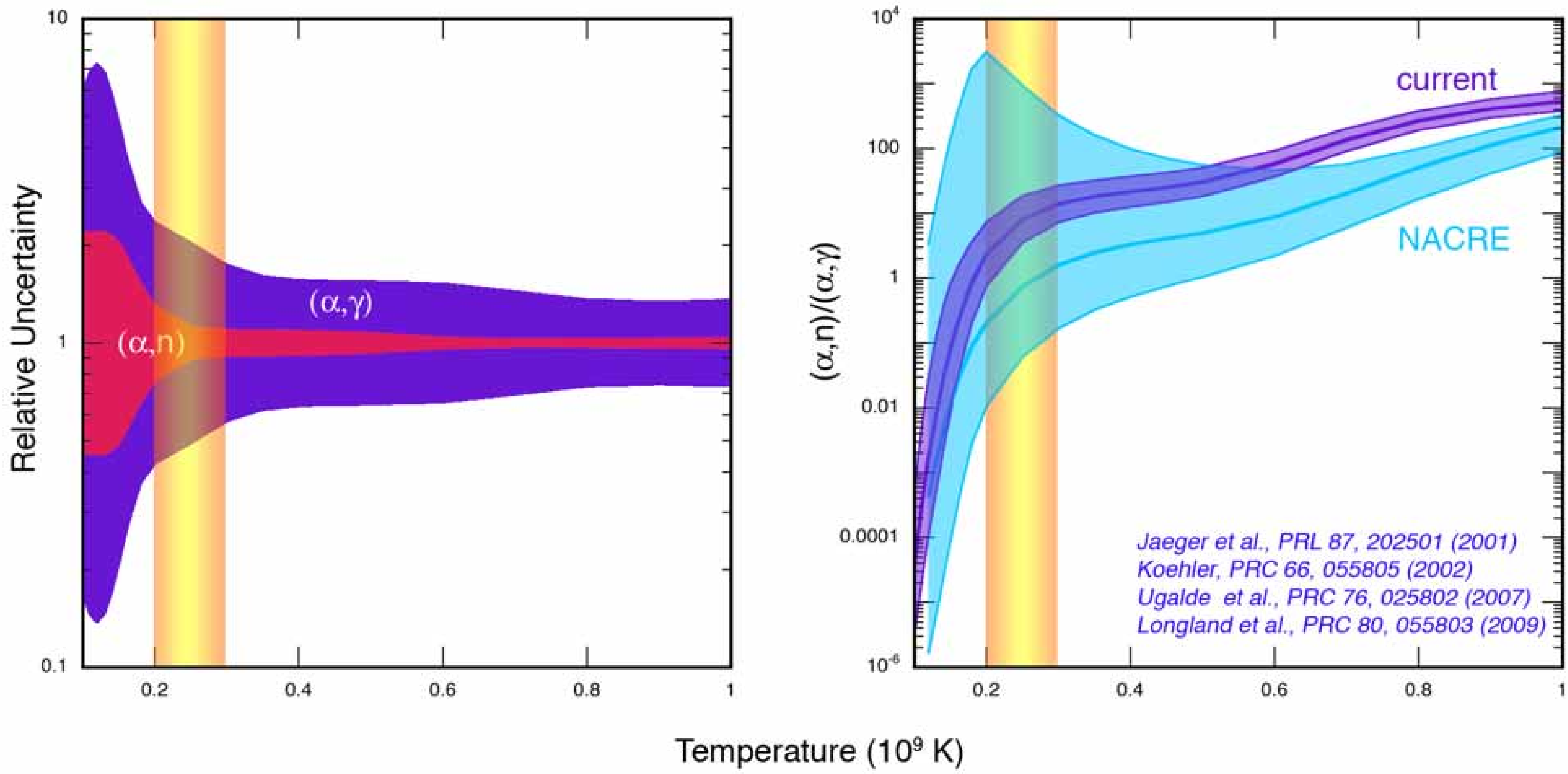

Issues: 3. n-capture cross sections for unstable targets (branch points)

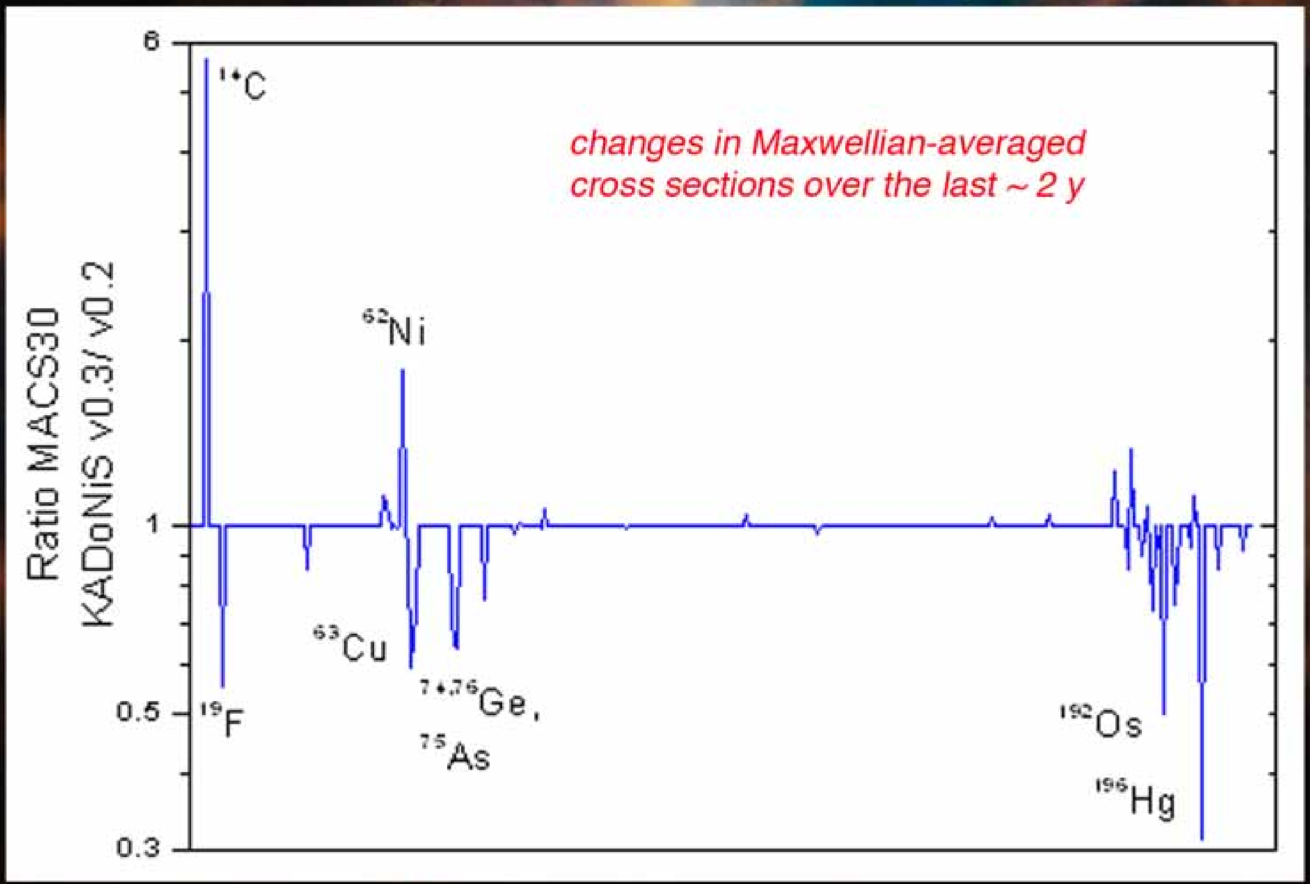

Issues: 3. n-capture cross sections for unstable targets (branch points)

4. effects of thermal excitation

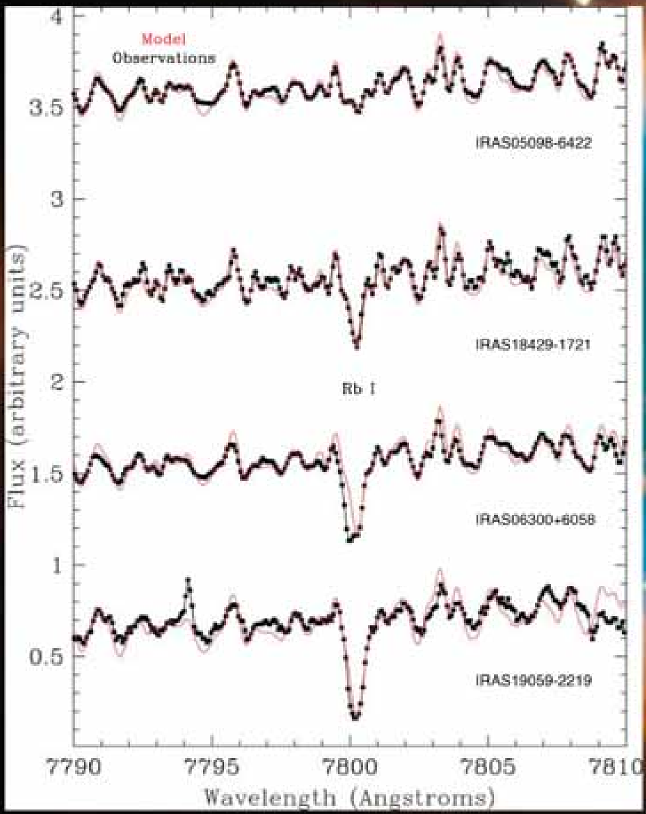

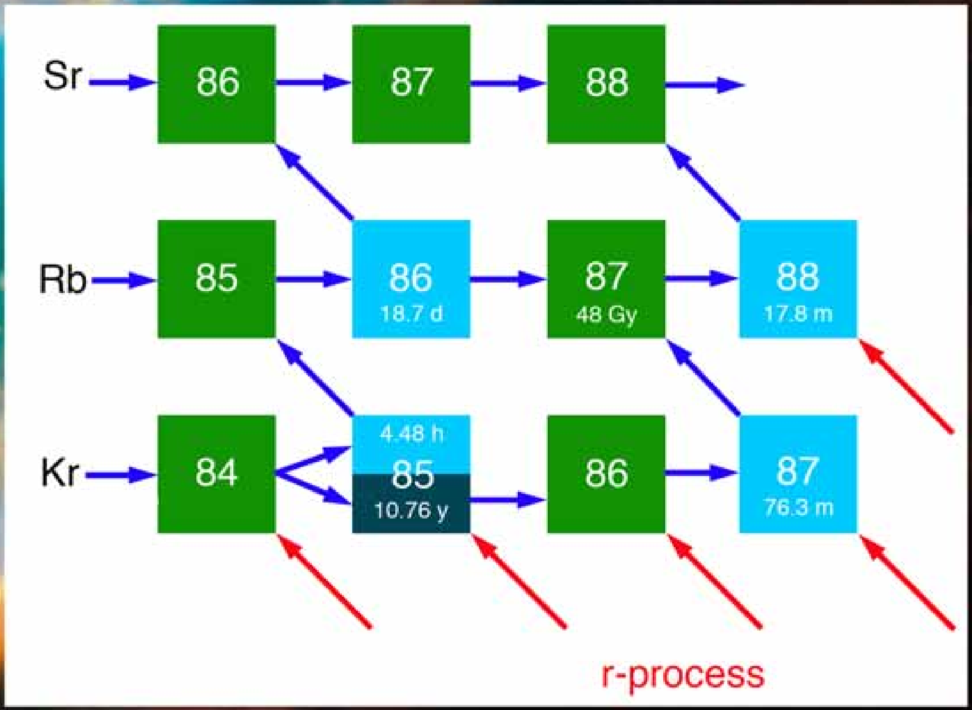

D.A. García-Hernández et al., Science **314**, 1751 (2006)

Observations of very metal-poor halo stars

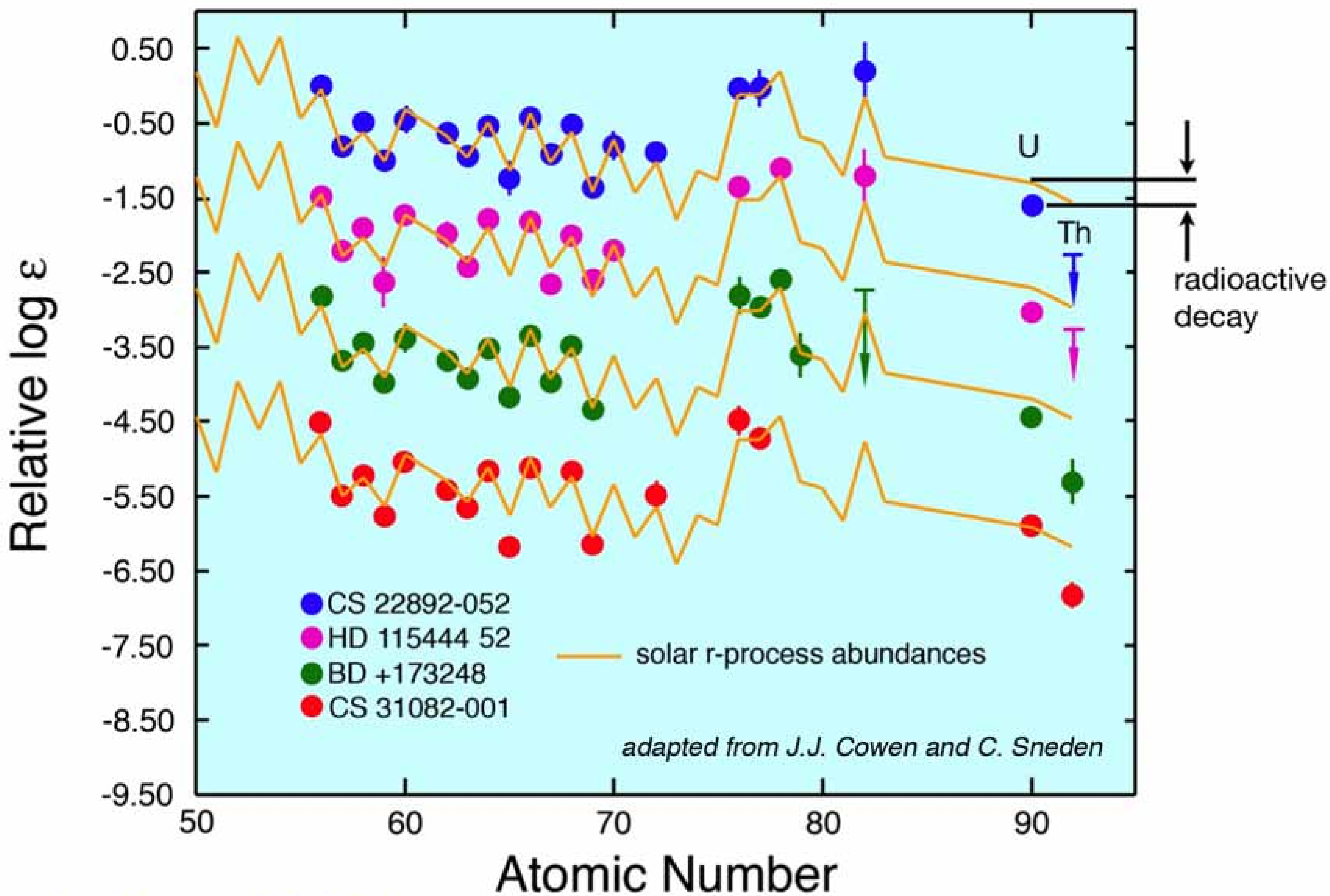

Eu-Th ages ~12 - 15 Gy

U-Th age = 14.1 ± 2.4 Gy [CS 31082-001, S. Wanajo *et al.*, Ap. J. **593**, 968 (2003)]

r-process nucleosynthesis

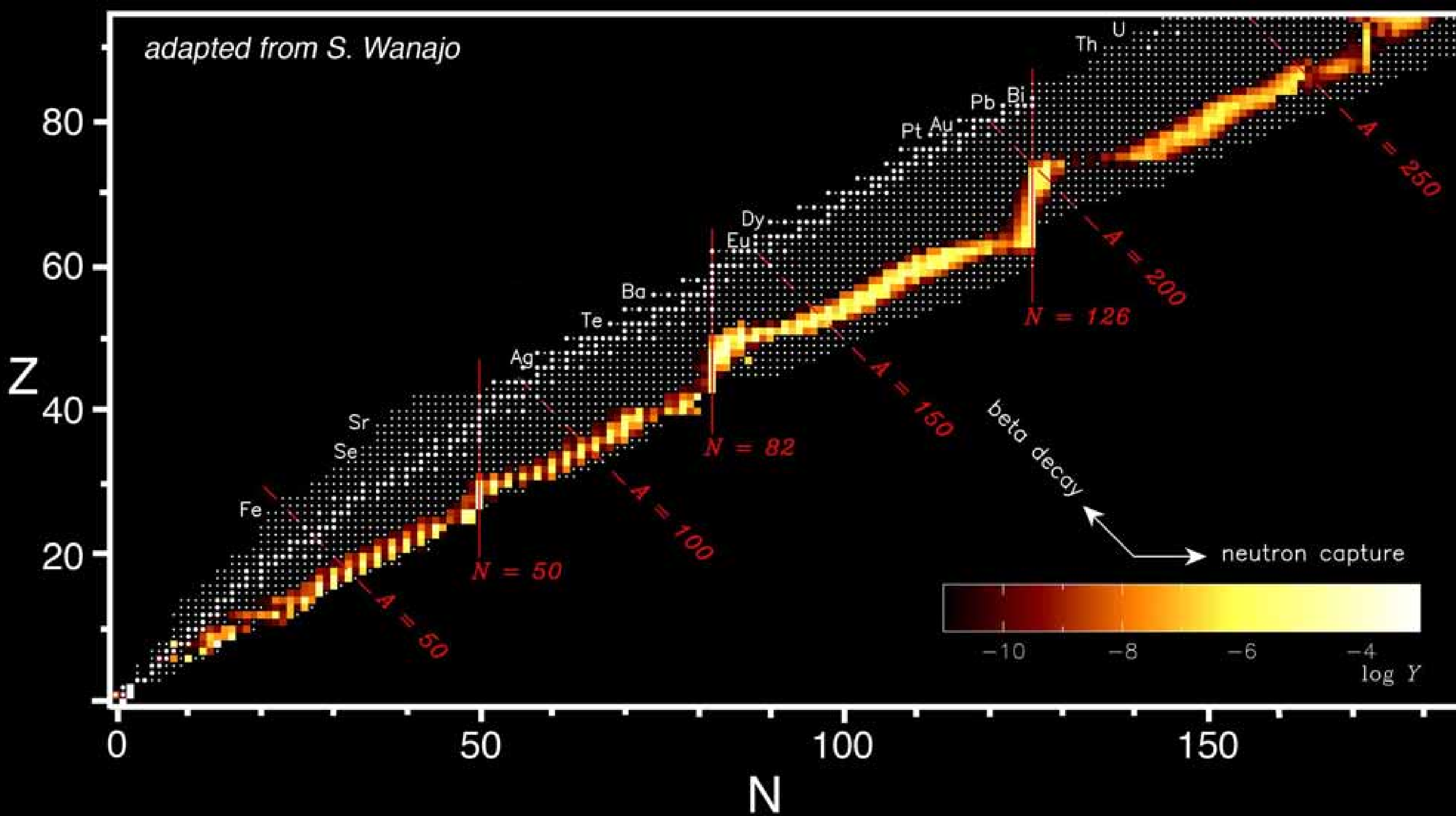

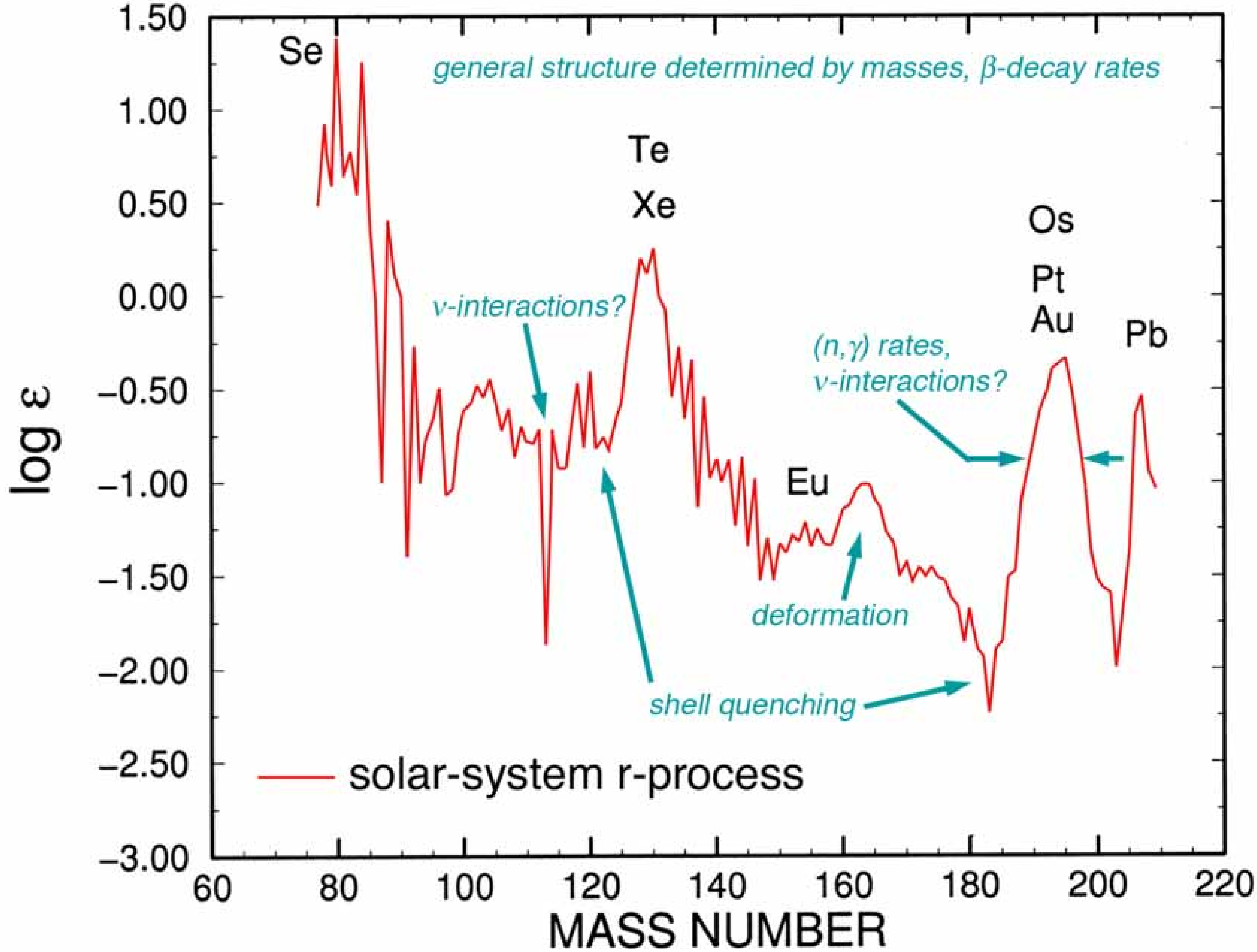

log ε
1.50
1.00
0.50
0.00
−0.50
−1.00
−1.50
−2.00
−2.50
−3.00
60
80
100
120
140
160
180
200
220
MASS NUMBER
Se
general structure determined by masses, β-decay rates
Te
Xe
Os
Pt
Au
Pb
ν-interactions?
(n,γ) rates,
ν-interactions?
Eu
deformation
shell quenching
solar-system r-process

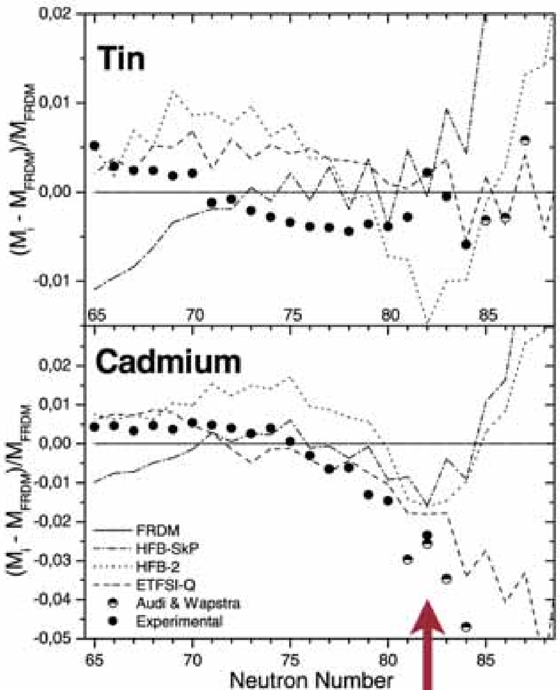

I. Dillmann et al., Phys. Rev. Lett. ***91****, 162503 (2003)*

evidence for shell quenching

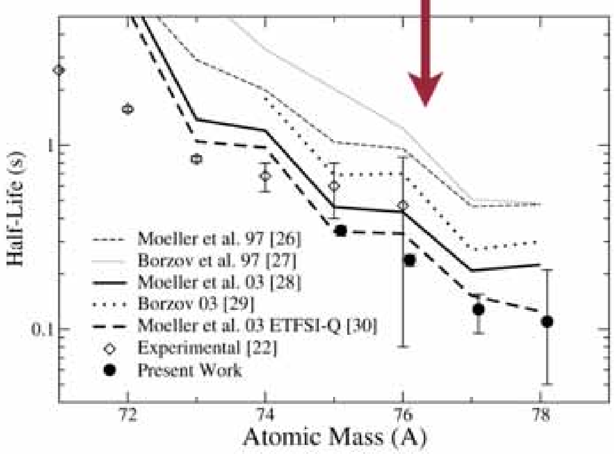

half-life of ^{78}Ni

[P.T. Hosmer et al.,
Phys. Rev. Lett ***94****, 112501 (2005)]*

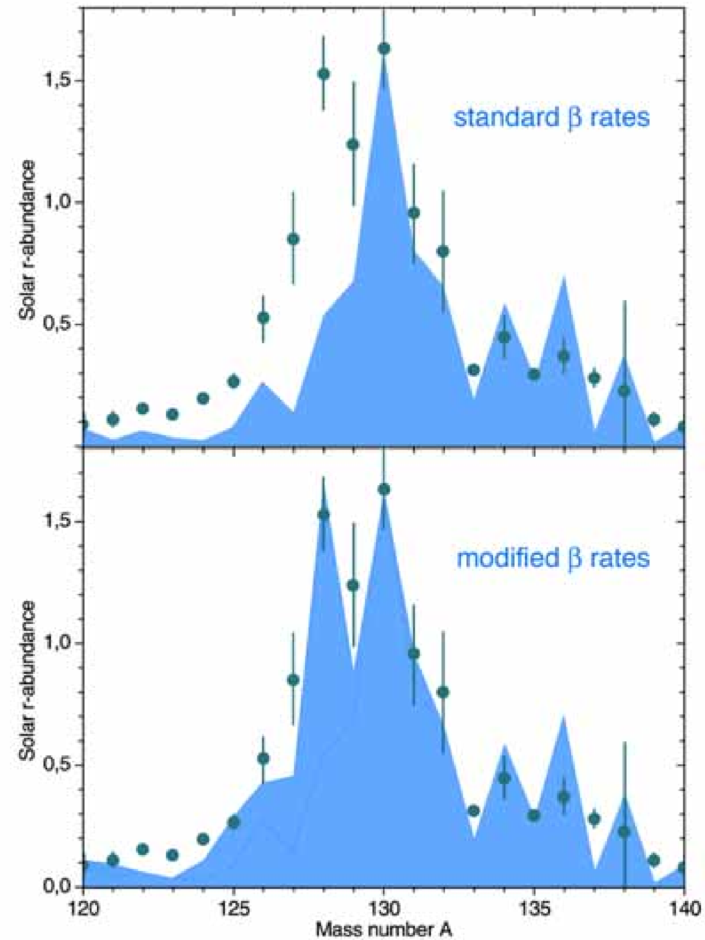

improved nuclear structure
no ν-interactions required

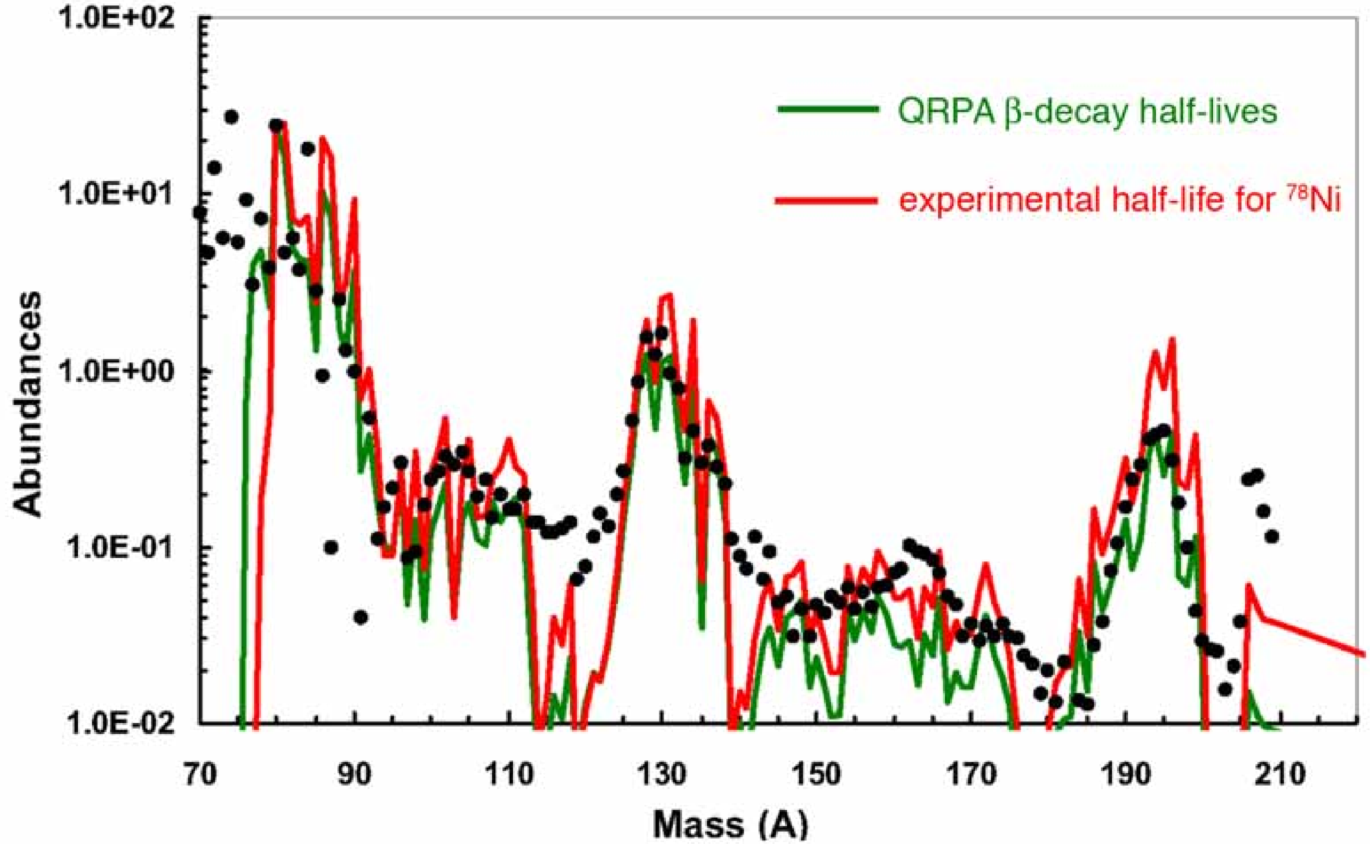

J. Pereira et al., arXiv:0901.1802v1 [nucl-ex] other effects, e.g. late-time (ν,n) reactions

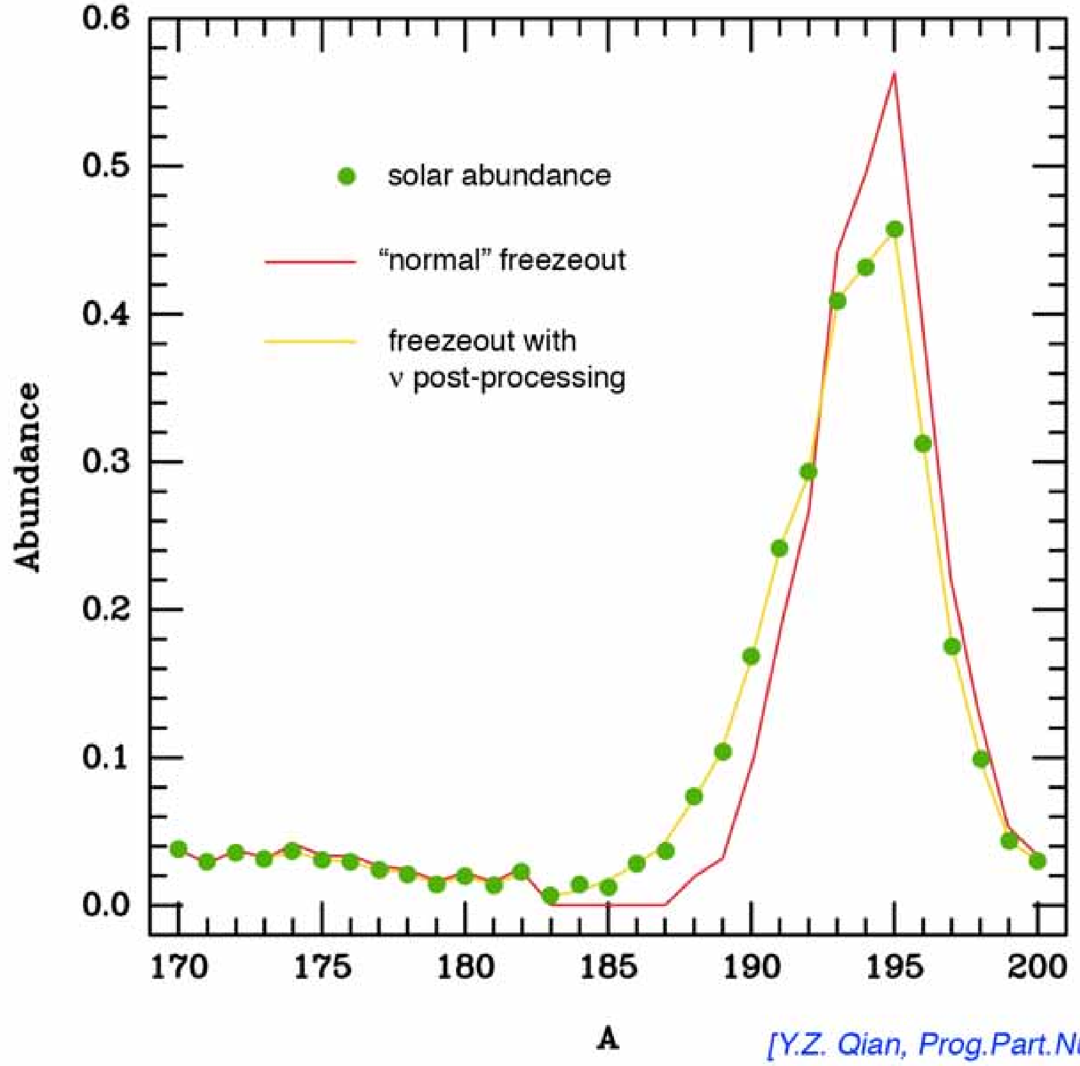

[Y.Z. Qian, Prog.Part.Nucl.Phys. **50**, 153 (2003)]

Masses and mass models

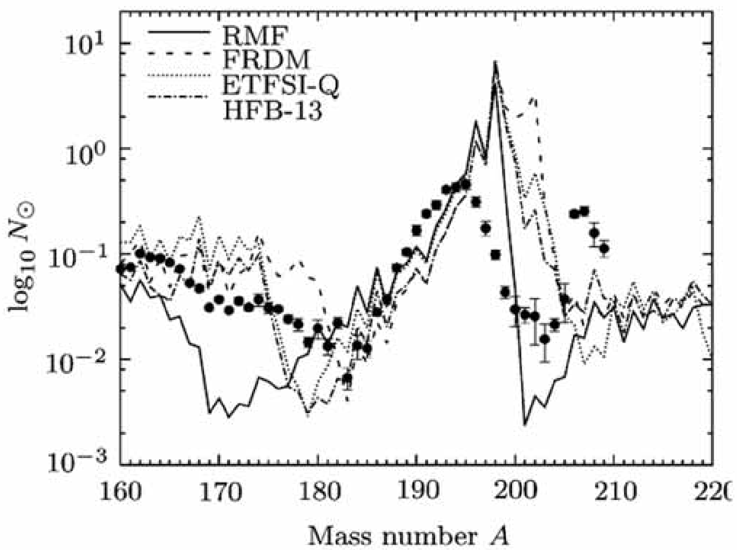

Fig. 2. Comparison of observed solar r-process abundances (filled circles) with theoretical abundance after β-decays calculated using RMF, FRDM, ETFSI-Q and HFB-13 mass models. The calculated abundances have been scaled to the solar r-process abundance at $A = 130$.

B.H. Sun and J. Meng, Chin. Phys. Lett. ***25*** *2429 (2008)*

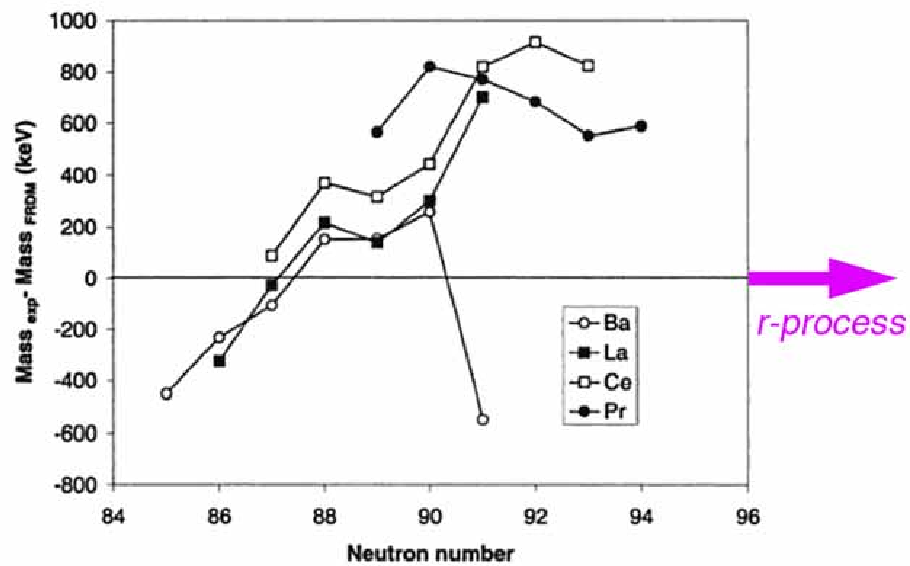

Figure 4. The differences between the masses measured by the CPT and those of the FRDM. The lines shown are to guide the eye only.

J.A. Clark et al. in "The r-process: The Astrophysical Origin of the Heavy Elements", Y.Z. Qian, E. Rehm, H. Schatz, F.-K. Thielemann, ed. (2004)

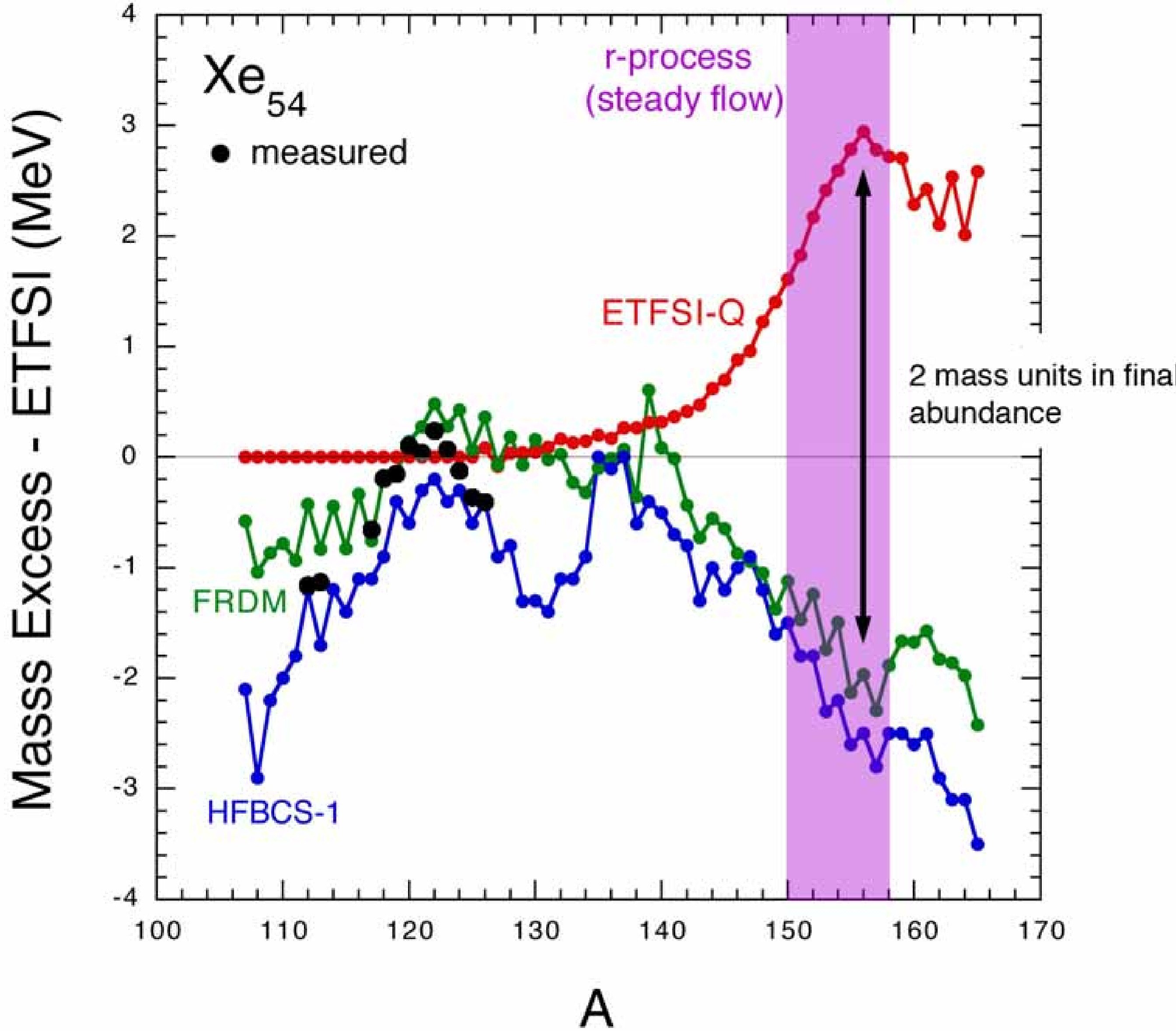

Xe54
measured
r-process
(steady flow)
ETFSI-Q
2 mass units in final
abundance
FRDM
HFBCS-1
Masss Excess - ETFSI (MeV)
A
4
3
2
1
0
-1
-2
-3
-4
100
110
120
130
140
150
160
170

A look ahead: **GSI**

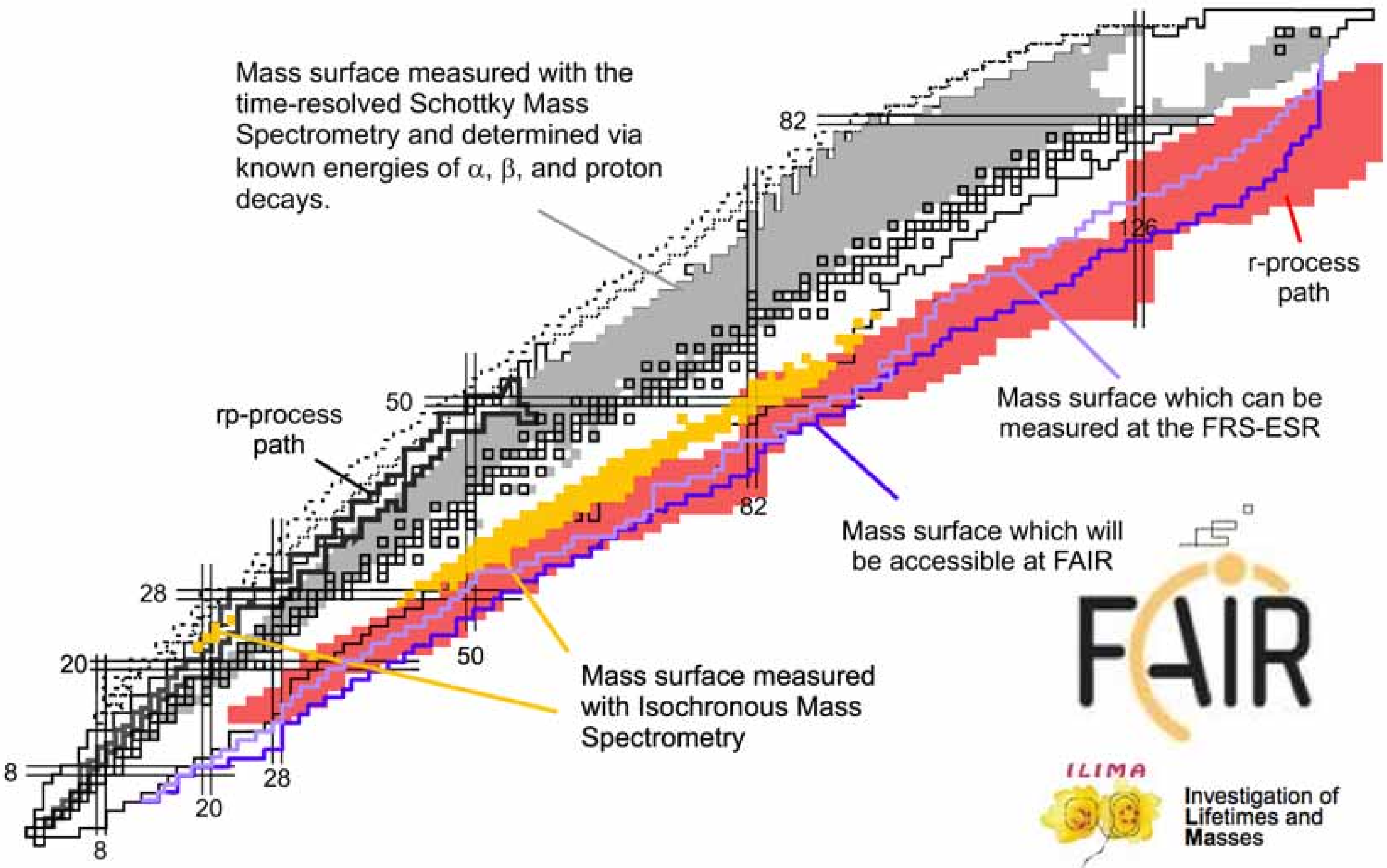

FAIR

ILIMA

Investigation of **L**ifetimes and **Ma**sses

Estimated beam intensity at BigRIPS

$^{86}Kr/^{136}Xe/^{238}U$ 1pμA

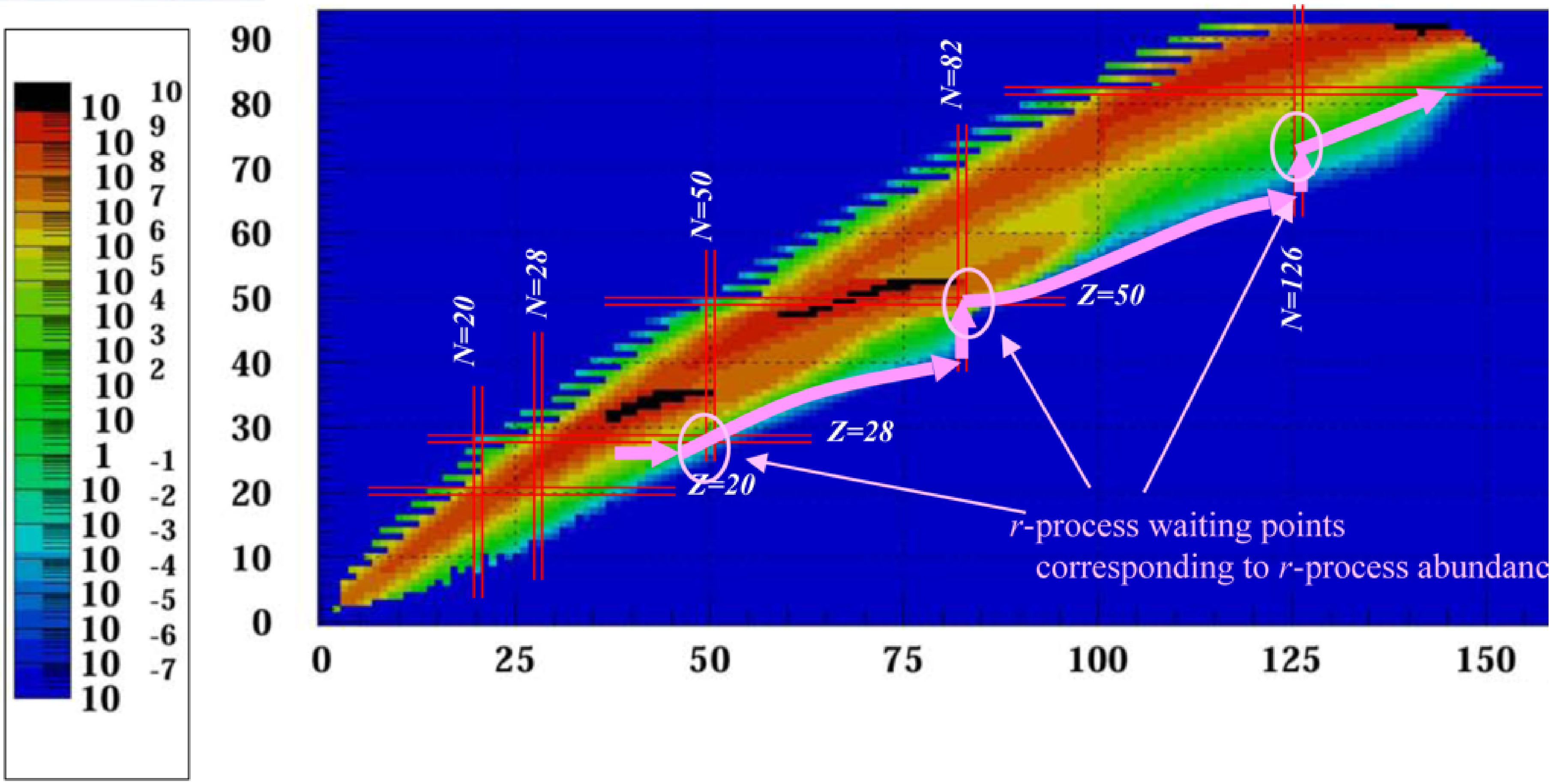

(adapted from T. Motobayashi)

New initiatives in the US

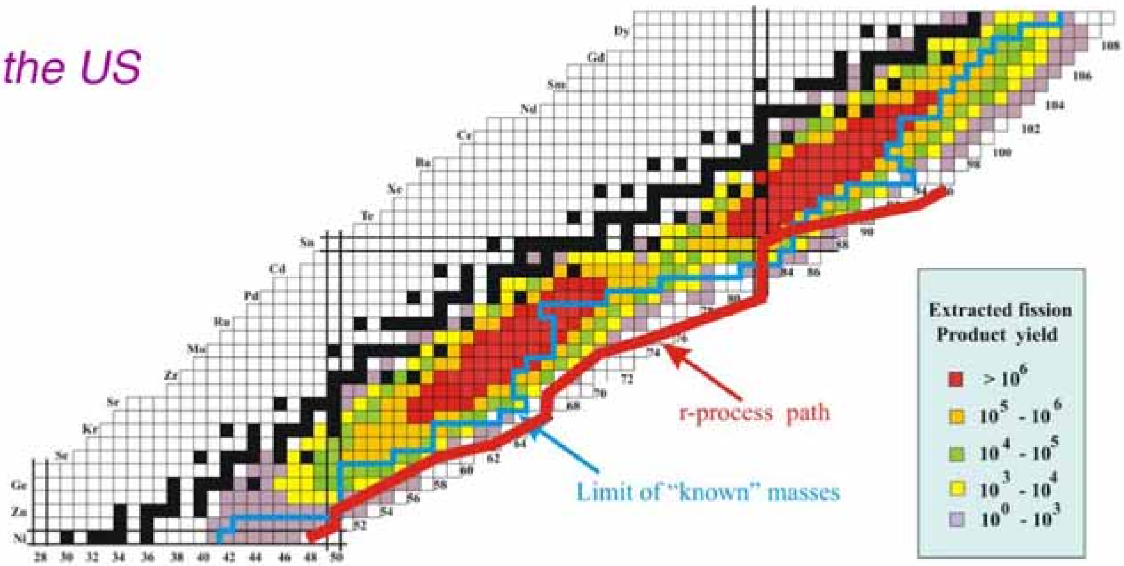

The CAlifornium Rare Isotope Breeder Upgrade (CARIBU - Argonne National Laboratory)

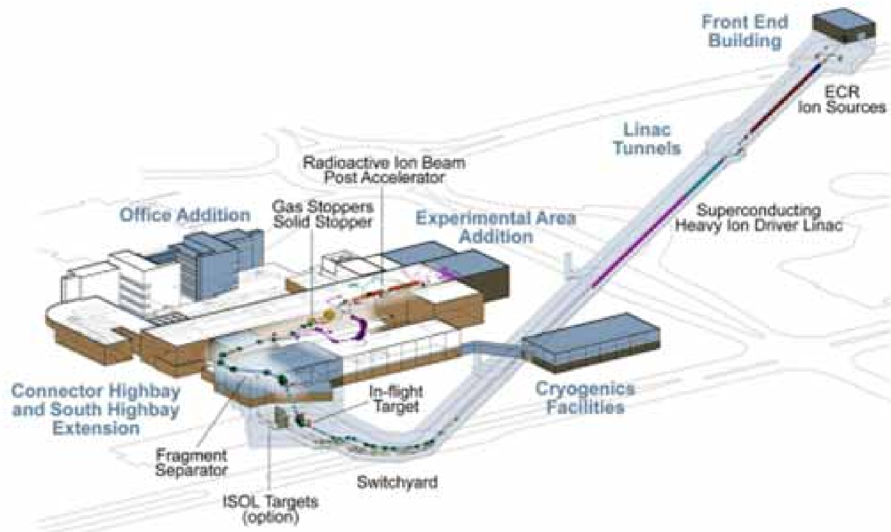

Facility for Rare Isotope Beams (FRIB - Michigan State University)

Reach of FRIB for r-process Studies

- β decay properties
- masses (Trap + TOF)
- (d,p) to constrain (n,γ)
- fission barriers, yields

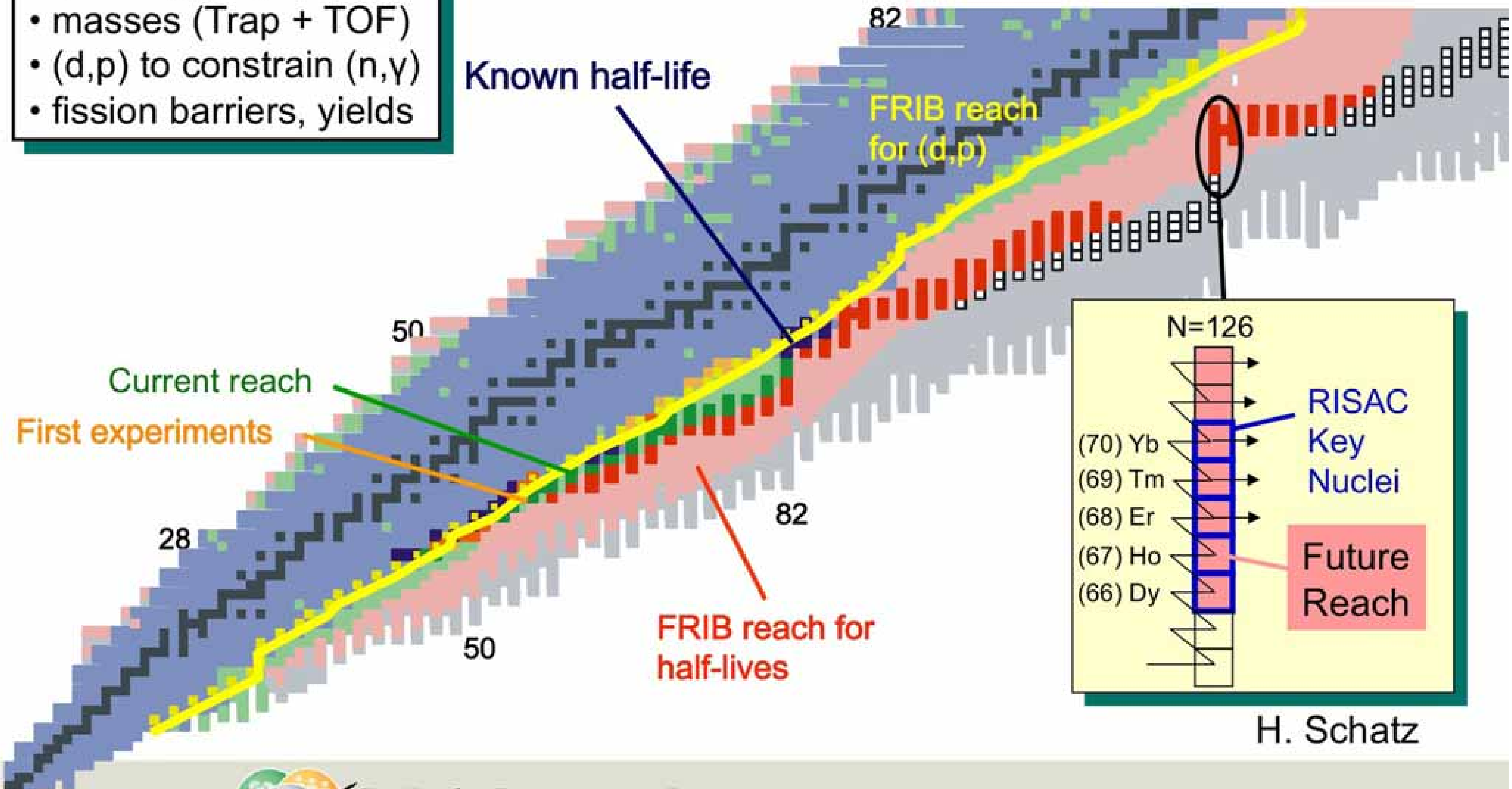

H. Schatz

another future facility: DIANA (Dakota Ion Accelerators for Nuclear Astrophysics)

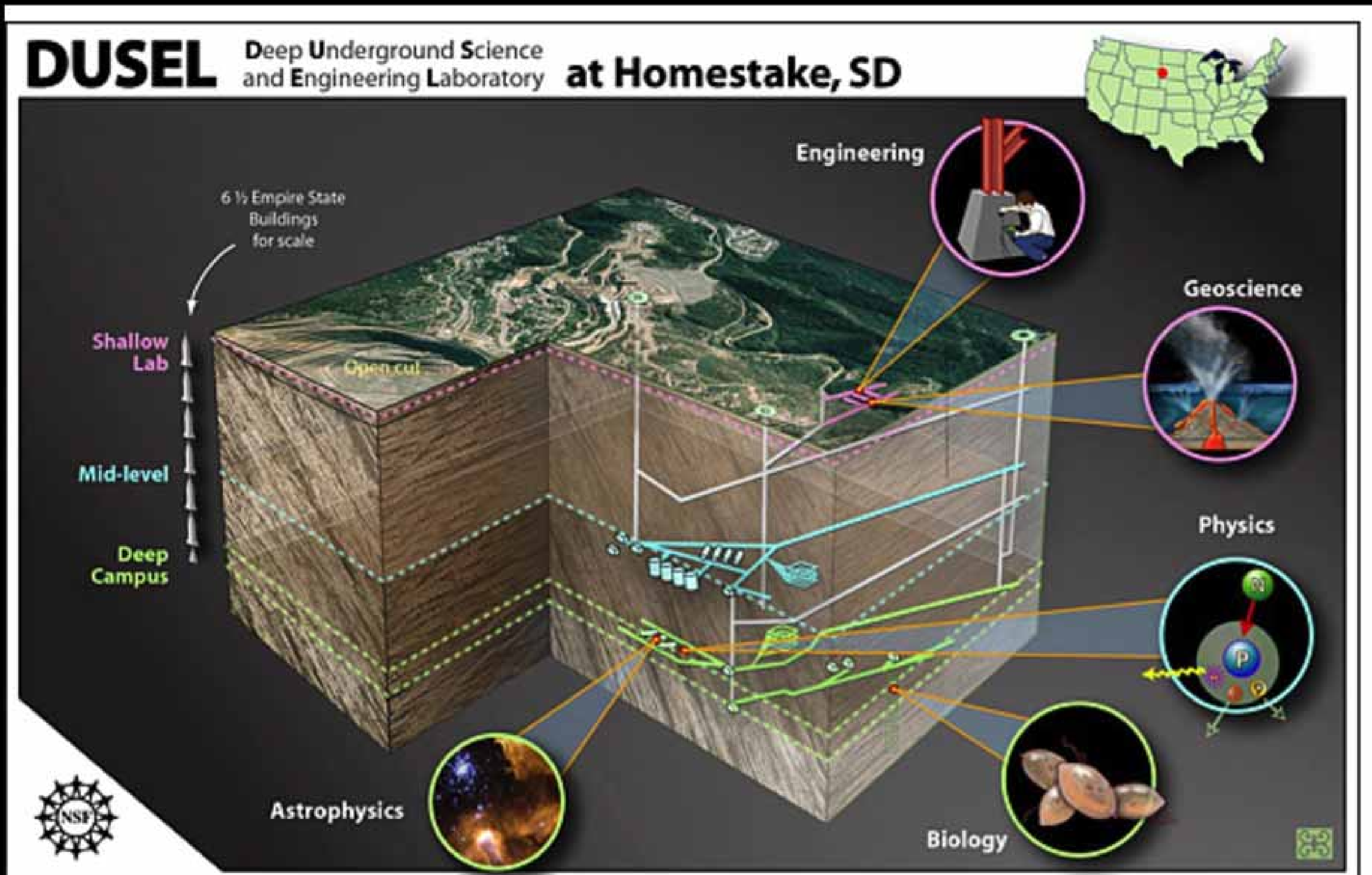

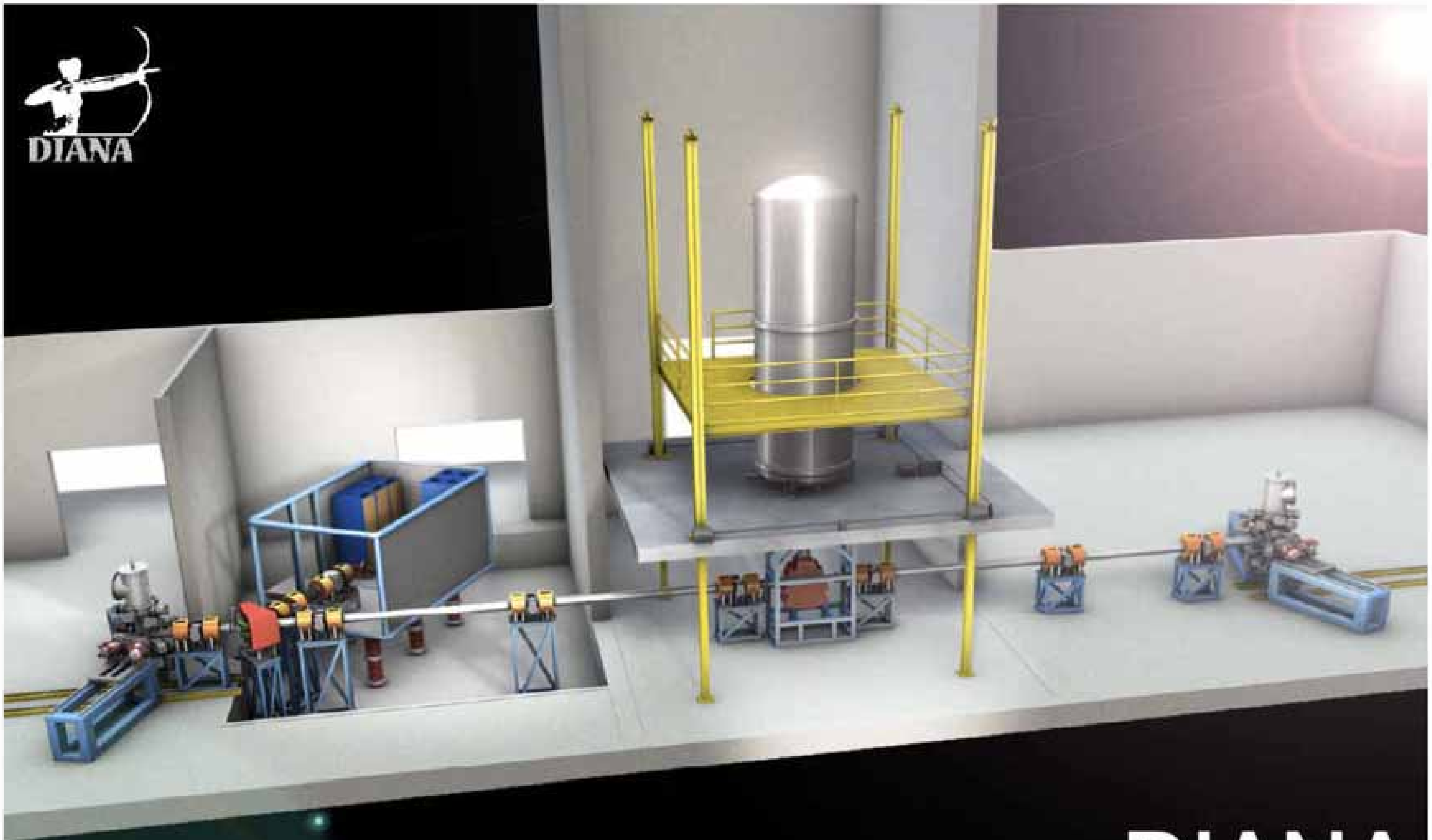

DIANA

A NOVEL NUCLEAR ASTROPHYSICS UNDERGROUND ACCELERATOR FACILITY

UNIVERSITY OF NOTRE DAME
THE UNIVERSITY of NORTH CAROLINA at CHAPEL HILL
COLORADO SCHOOL OF MINES
BERKELEY LAB
ERNEST ORLANDO LAWRENCE BERKELEY NATIONAL LABORATORY